Spatial and temporal variability in attenuation of polar organic micropollutants in an urban lowland stream

Anna Jaeger, Malte Posselt, Andrea Betterle, Jonas Schaper, Jonas Mechelke, Claudia Coll, and Jörg Lewandowski

DOI
10.1021/acs.est.8b05488

Original publication date
13 February 2019 (Available online)

Document version
Accepted manuscript

Published in
Environmental Science and Technology

Citation
Jaeger A, Posselt M, Betterle A, Schaper J, Mechelke J, Coll C, Lewandowski J. Spatial and temporal variability in attenuation of polar organic micropollutants in an urban lowland stream. Environ Sci Technol. 2019.

Spatial and temporal variability in attenuation of polar organic micropollutants in an urban lowland stream

Jaeger Anna*‡(1,2), Posselt Malte‡ (3), Betterle Andrea (4,5,6), Schaper Jonas (1,7), Mechelke Jonas (4,8), Coll Claudia (3), Lewandowski Joerg (1,2)

‡These authors contributed equally to the work

*corresponding author: anna.jaeger@igb-berlin.de, Leibniz-Institute of Freshwater Ecology and Inland Fisheries, Department Ecohydrology, Müggelseedamm 310, 12587 Berlin, Germany

(1) Leibniz-Institute of Freshwater Ecology and Inland Fisheries, Department Ecohydrology, Berlin, Germany

(2) Humboldt University Berlin, Geography Department, Berlin, Germany

(3) Stockholm University, Department of Environmental Science and Analytical Chemistry, Stockholm, Sweden

(4) Eawag, Swiss Federal Institute of Aquatic Science and Technology, Department of Water Resources and Drinking Water, Dübendorf, Switzerland

(5) University of Neuchâtel, Centre of Hydrogeology and Geothermics, Neuchâtel, Switzerland

(6) University of Padova, Department of ICEA and International Center for Hydrology, Padua, Italy

(7) Technical University of Berlin, Chair of Water Quality Engineering, Berlin, Germany

(8) ETH Zürich, Institute of Biogeochemistry and Pollutant Dynamics, Zürich, Switzerland

Abstract

Contamination of rivers by trace organic compounds (TrOCs) poses a risk for aquatic ecosystems and drinking water quality. Spatially- and temporally-varying environmental conditions are expected to play a major role in controlling in-stream attenuation of TrOCs. This variability is rarely captured by in situ studies of TrOC attenuation. Instead, snap-shots or time-weighted average conditions and corresponding attenuation rates are reported. The present work sought to investigate this variability and factors

controlling it by analysis of 24 TrOCs over a 4.7 km reach of the River Erpe (Berlin, Germany). The factors investigated included sunlight and water temperature as well as the presence of macrophytes. Attenuation rate constants in 48 consecutive hourly water parcels were tracked along two contiguous river sections of different characteristics. Section 1 was less shaded and more densely covered with submerged macrophytes compared to section 2. The sampling campaign was repeated after macrophyte removal from section 1. The findings show, that section 1 generally provided more favorable conditions for both photo- and biodegradation. Macrophyte removal enhanced photolysis of some compounds (e.g. hydrochlorothiazide and diclofenac) while reducing the biodegradation of metoprolol. The transformation products metoprolol acid and valsartan acid were formed along the reach under all conditions.

TOC Art

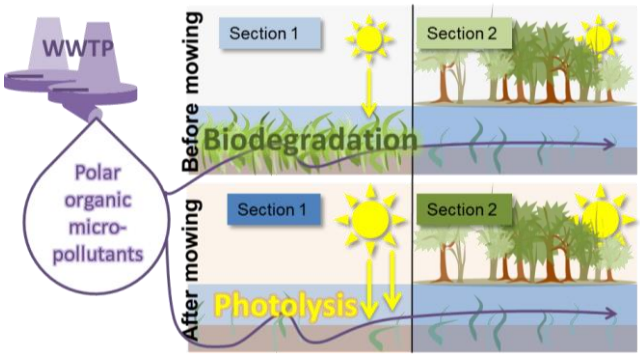

Introduction

Polar trace organic compounds (TrOCs), such as pharmaceuticals and personal care products, as well as their transformation products (TPs) are frequently detected in urban streams receiving wastewater treatment plant (WWTP) effluent.[1-5] TrOCs have been described to impair aquatic ecosystem functioning and can pose a risk to drinking water quality, particularly in semi-closed urban water cycles.[6-8] Despite their widespread occurrence, TrOCs remain mostly unregulated and knowledge about their fate in streams is still limited.[4,9-11]

Biodegradation, photolysis and sorption are among the key processes controlling TrOC fate in freshwaters. These processes are usually studied in laboratory experiments under controlled conditions.[12-17] The occurrence of processes in situ, however, depends on a diverse set of environmental conditions.[18] Biodegradation is driven by factors, such as the composition of the microbial community, water temperature, redox zonation and availability of ecohydrological interfaces.[15,19,20,21] Likewise, photolysis is not only controlled by intensity of solar radiation but also by, e.g. shading and concentration of dissolved organic carbon (DOC).[22,23] Sorption depends on availability of binding sites on organic matter, sediment particles or biofilm, for example.[24,25] On one hand, this multitude of environmental conditions may vary temporally, e.g. diurnal and annual fluctuations in temperature. On the other hand, conditions may vary spatially within a river, e.g. in transient storage zones where water is delayed in its downstream transport and contact with ecohydrological interfaces is increased. Examples for transient storage zones are hyporheic zones, groyne fields, dead zones behind obstacles and vegetation, and near-shore pools of stagnant water.[26,27]

Submerged macrophytes are an important factor which controls environmental conditions in rivers. They provide a range of ecosystem services, such as creating diverse habitats for fish and invertebrates. They influence oxygen and nutrient concentrations and can change flow velocities and sediment morphology.[28,29] Macrophytes also alter shading and thermal regimes and create transient storage

zones.[26,27] Furthermore, they are known to have a direct removal function for TrOCs through biodegradation on epiphytic biofilm or plant uptake.[30] Despite their important role for river ecosystems, removal of aquatic vegetation from rivers is a common management technique for flood prevention.[29] Some rivers are even mowed several times a year.[28] Due to their intense impact on in-stream conditions and their pollutant removal functions, we expect that macrophytes play a major role in in-stream attenuation of TrOCs and that their removal changes the fate of TrOCs drastically.[26,29-31]

The spatial and temporal heterogeneity of drivers of attenuation processes makes in situ investigation of TrOC in-stream fate generally challenging. Some important in-stream attenuation studies have been conducted previously in single rivers implementing different methods. Some followed a single water parcel in a Lagrangian sampling scheme.[32-34] In those cases snap-shots of attenuation condition and corresponding attenuation values are reported. Others investigate attenuation over longer periods, mostly resulting in time-integrated single attenuation values.[35-37] While such studies provide important quantitative information about attenuation or potential persistence of TrOCs in streams, the identification of processes and environmental drivers remains difficult due to a low comparability between studies. Two studies attempted to enhance comparability by conducting the same sampling methods and measuring the same set of parameters at four different rivers.[38,39] However, the boundary conditions between rivers, such as discharge, sediment characteristics or portion of effluent differed to a point where it hindered the identification of distinct processes and responsible drivers.

The objective of the present study was to investigate within-stream variability of TrOC fate, i.e. the change of TrOC attenuation or transformation in time or space within one single stream. We suggest that this approach has two major advantages: Firstly, for each compound a distribution of rate constants is obtained as opposed to a single value, making the result more realistic and promoting comparability to other studies. Secondly, it facilitates identification of processes and related drivers that influence the fate of individual compounds due to a higher conformity in the remaining boundary conditions within

88 one stream than between different streams. Hanamoto et al.[40] are to our knowledge the first to
89 demonstrate diurnal changes of in-stream attenuation in an hourly resolution leading to the
90 identification of diurnal fluctuation in solar radiation as a major control for attenuation of certain
91 compounds in situ.

92 In the present work we studied the in-stream fate of a set of 24 TrOCs and TPs. We expected that
93 temporally and spatially varying environmental conditions would lead to a variation in attenuation rate
94 constants of compounds that undergo biodegradation, photolysis or sorption and attempted to identify
95 the underlying processes. We hypothesized that TrOC attenuation will: a) differ between two adjacent
96 sections of different characteristics; b) change after removal of macrophytes from the first section; c)
97 depend on diurnal fluctuations in environmental conditions, such as water temperature or solar
98 radiation.

99

100 **Material and Methods**

101 *Study site*

102 The experiment was conducted in the River Erpe, a lowland stream located east of Berlin, Germany. The
103 study reach was 4.7 km in length, starting 0.7 km downstream of the outlet of WWTP Münchehofe and
104 ending 0.8 km prior to the mouth of the River Erpe into the River Spree (Figure 1). During the study
105 period, the WWTP discharged on average (±SD) 0.44 ± 0.22 $m^3 s^{-1}$ treated wastewater into the river (data
106 provided by WWTP Münchehofe, Berlin) increasing its discharge to 0.69 ± 0.21 $m^3 s^{-1}$ at the start of the
107 study reach in daily fluctuations (Figure S1). The effluent strongly influences the hydrological regime and
108 the chemical composition of the study reach.[41] It was divided into two sections (S1 and S2) of 1.6 km and
109 3.1 km length, respectively, by three sampling stations (stations A, B and C; Figure 1). Google-maps
110 satellite images showing maximum foliage were used to obtain the portions of shading of the river

surface in the different sections. S1 was almost continuously exposed to solar radiation (5% direct shading). Consequently, macrophytes populated the complete channel of S1 with total dry biomass (±SD) of 176 ± 87.3 g m^{-2} (80% *Stuckenia pectinata*, 12% *Callitriche* sp., 8% *Sparganium emersum*). The channel of S2, in contrast, is 58% directly shaded by adjacent trees and thus the abundance of macrophytes was generally low. Due to patchiness it was not feasible to measure the average biomass. However, since macrophyte biomass is highly sunlight dependent,[42] we estimated that the difference in macrophyte biomass density was similar to the difference in sunlight-exposed channel area between the sections (S1 95%: S2 42%). Thus we speculate that the average dry biomass density in S2 was roughly 0.44 of the dry biomass in S1 (~ 78 g m^{-2}). Most of the river's sediment has a high organic matter content, and thus low hydraulic conductivity. Only in the first 400 m of S1, the river is connected to the fine sandy aquifer and characterized as a losing stream.[43] Infiltration of river water to the hyporheic zone in this stretch was previously measured by means of vertical temperature profiles.[44] Although re-exfiltration of hyporheic water to the river has not been examined, hyporheic exchange flow is probable where dunes form and at the two fish ladders in this stretch. Additionally, a small side channel diverts from the main channel in S1 40 m downstream of station A and re-enters the river at two locations: 641 and 176 m upstream of station B. Similar to the effect of the potential hyporheic zone, its effect is accounted to a lumped transient storage zone of unknown extent. The channel of S2 in contrast is predominantly muddy, and thus mostly confined.[43] The size of the transient storage zone was not quantified, but due to the side channel, the macrophytes and the sediment characteristics described above, it is expected to be larger in S1 than in S2. Detailed information about background data, such as discharge, water chemistry and meteorological data are shown in the Supplementary Information (SI).

Sampling

Autosamplers (ISCO 3700 portable sampler, Teledyne Isco, Lincoln NE) were installed at stations A, B and C collecting surface water from the center of the stream cross-section. Samples were continuously

cooled inside the autosamplers by ice-packages. A set of 48 hourly samples was taken twice at each station: before (*bm*) and after (*am*) macrophytes removal from the riverbed of S1. A delay of a daily reoccurring electrical conductivity (EC) trough served as an approximation for travel times between stations. We estimated the travel times from time series in EC of the day before sampling, both *am* and *bm*. Hence, to capture the water parcels most efficiently, the autosampler at station A started sampling at 23:00 on the 14.06.2016 (*bm*), while sampling at stations B and C followed 4 and 8 hours later, respectively. On the 17.06.2016, S1 was mowed to clear the water body from macrophytes. Trucks with mowing shovels cut the plants off the streambed and shoveled them to the shore (Figure S2). The delay of the EC trough after mowing showed that the travel time in S1 was reduced by roughly 1 hour, while the travel time in section 2 remained similar to before mowing. Hence, the first sample after mowing was taken at station A on the 21.06.2016 at 14:00, followed by station B and C, 3 and 7 hours later, respectively. All water samples were split into subsamples for respective analytical methods and stored accordingly until processing. In addition to autosamplers, Chemcatcher® passive samplers in polar configuration were deployed in duplicates at all stations *bm* (11 days, 05.06. to 16.06.2016) and *am* (10 days, 20.6. to 30.6.2016).[45] Details on the passive sampler procedure can be found in the SI.

Collecting of meteorological, biomass, shade cover and electrical conductivity data

Global solar radiation and precipitation data were recorded continuously at a weather station (IGB Berlin) located approximately 2.6 km south-east of sampling station B. At each sampling station data-loggers (CTD-Diver, van Essen Instruments, Delft, the Netherlands) were set up close to the sampling-tubes to track EC, water stage and water temperature continuously (5 minute intervals). Background data during the sampling periods are shown in Figure S1. To estimate the average biomass of macrophytes *bm* in S1, plants from three representative 4 m^2 sites ca 200 m downstream of station A were manually collected. The species were identified and separately dried to obtain dry biomasses.

Quantitative determination of TrOCs and boron

TrOC analysis of all water samples was conducted at Stockholm University, Sweden.[46] Prior to analysis samples were defrosted, vortexed, combined with MeOH and internal standard mix, vortexed again and finally filtered (0.45 µm, PES membrane). Concentrations of 24 TrOCs (a full list is provided in Table 1) were determined by direct injection ultra-high performance liquid chromatography tandem mass spectrometry as described by Posselt et al.[46] . Intermediate precision was good (repeatability <24% RSD and reproducibility <18% RSD) and method accuracy excellent for most compounds.[46] Details on quality control of TrOC analysis are described in the SI and further data including spike/recovery experiments with Erpe water can be found in Posselt et al.[46]. Concentration levels of all target compounds in all Erpe samples were above the limit of detection. Values below limit of quantification (LOQ) were only found for α-hydroxymetoprolol, carbamazepine-10,11-epoxide and sulfamethoxazole and were replaced by $LOQ \cdot 2^{-0.5}$ (<25% of samples).

Subsamples for analysis of boron were filtered immediately after sampling (0.45 µm cellulose acetate), acidified with HCl, stored at 4 °C and measured by inductively coupled plasma optical emission spectrometry (ICP iCAP 6000series, Thermo-Fisher-Scientific Inc.).

Analysis of TrOCs collected in the passive samplers was conducted at EAWAG Zurich, Switzerland, by an established liquid chromatography high-resolution tandem mass spectrometry method for passive samplers (see SI for details). It included 17 out of the 24 compounds measured in the water samples (Table S4).[45] Concentrations were calculated using experimentally determined sampling rates (data not shown).

Travel times estimated by deconvolution of intrinsic electrical conductivity signals

The daily dynamics of the WWTP discharge cause a relatively regular diurnal fluctuation in electrical conductivity (EC) in the river downstream of the wastewater outlet (e.g.: station A *bm*: 811-1170 µS cm^{-1}; *am*: 994-1150 µS cm^{-1}; Figure S4). EC is assumed to behave conservatively in the surface water, i.e. the

signal is not affected by biological or chemical processes but merely by advection and dispersion.[47,48] Thus, EC can serve as tracer for solute transport and allows determination of travel times between sampling stations. Water residence time distributions between pairs of sampling stations were estimated using a non-parametric deconvolution method for EC time series (see SI).[49,50] Given the strong daily periodicity of the input EC signals, the estimation of the transfer function was limited to one day. The duration was sufficient to capture the bulk of the transfer function and to prevent secondary peaks resulting from the 24 h periodicity of the input EC signal. A period of 4 days from 13.06.16 8:00 to 17.06.16 7:55 and from 21.06.2016 14:00 to 25.06.2016 13:55 was considered (i.e. *bm* and *am*) to estimate the residence time distributions. Peak travel times were estimated to be 4.4 h in S1bm, 3.1 h in S1am, 4.5 h in S2bm and 5.4 h in S2am.

Calculation of TrOC attenuation rate constants

In order to track changes in solute concentration along a river section hourly consecutive water parcels were monitored following the idea of a Lagrangian sampling scheme.[33,47] The concentration at the start time of the parcel (p) of a solute (x) at the upstream station ($C_{p,x,in}$) is compared to the concentration at the start time plus the travel time (t_p) at the downstream station ($C_{p,x,out}$). To account for the possible influence of dilution during the travel period of a parcel, the change of concentration is corrected by the change of concentration in a conservative WWTP-derived reference compound, in this case boron.[51] Low changes in boron concentrations between stations revealed that dilution was generally of minor importance (Figure S5). The concentrations and the C_{ref}:C_x ratios in each sample are assumed to represent the concentrations during the passing-time of one parcel (1 h) at each station. To calculate the attenuation rate constants ($k_{att,p,x}$), pseudo first-order reactions were assumed for all compounds.[17,18,39,40]

$$k_{att,p,x} = \ln\left(\frac{\frac{c_{p,x,in}}{c_{p,x,out}}}{\frac{c_{p,ref,in}}{c_{p,ref,out}}}\right)/t_i \qquad (1)$$

Consequently, k_{att} in S1 were calculated from concentrations at stations A (C_{in}) and B (C_{out}), while k_{att} in S2 were calculated from concentrations at stations B (C_{in}) and C (C_{out}). In order to assess the influence of spatial and temporal differing environmental conditions on k_{att} of individual compounds, we compare the distributions of k_{att} temporally, i.e. *bm* and *am*, and spatially, i.e. in S1 and in S2. This leads to a division into 4 different conditions: S1bm (n=48), S1am (n=47), S2bm (n=47) and S2am (n=46), which we refer to as "sampling situations" in the present work. The calculation of average solar radiation during a water parcel's travel period and the average water temperature a water parcel is exposed to is shown in the SI.

Statistical methods

Since environmental conditions are often not linearly related to k_{att},[22] Spearman rank correlations (ρ) were applied to determine the correlation of k_{att} with solar radiation and water temperature. Kruskal-Wallis tests in combination with Conover tests[52] (post-hoc pairwise test for multiple comparisons of mean rank sums) including two-stage linear step-up p-value correction as described by Benjamini et al.[53] were implemented to identify significant differences in distributions of k_{att} between sampling situations (Table S2). This ranked non-parametric test was used, because according to Shapiro-Wilk tests normality was not given in all distributions (Table S2). The significance levels (p) for the correlations and the comparisons were set to 5%.

Results and discussion

TrOC concentrations and attenuation rate constants

In general, TrOC concentrations at station A followed the discharge dynamics of the WWTP and showed diurnal fluctuations: For most TrOCs, low concentrations were observed around 7:00am. Highest concentrations were usually observed in the afternoon (Figure S5). Generally concentrations found in River Erpe were comparably high. Average concentrations at station A exceeded the average

227 concentrations measured in an EU-wide survey of 90 WWTP effluents for 1H-benzotriazole,
228 carbamazepine, venlafaxine, irbesartan, tramadol and the maximum measured concentrations for
229 bezafibrate and diclofenac.[4] Guanylurea, valsartan and 1H-benzotriazole were the most abundant
230 compounds with average concentrations (min-max) of 68.8 (46-90) µg L^{-1}, 28.5 (17-38) µg L^{-1} and 10.7
231 (5.5-18) µg L^{-1} at station A (n=96), respectively (Table 1). These compounds were measured in the µg-
232 range in river water previously.[3,39,54] TrOC concentrations of the 17 compounds estimated by passive
233 samplers (10- and 11-day time-weighted averages) were in the same order of magnitude as those
234 measured by active sampling (Table S4). As expected, the medians and the distributions of k_{att} are
235 compound-specific and may vary significantly between sampling situations. The highest median k_{att} was
236 found for 4-hydroxydiclofenac in S1am (0.14 h^{-1}, interquartile range (IQR) 0.30 h^{-1}). Continuous formation
237 along the river sections was observed for metoprolol acid and valsartan acid as median net-k_{att} values
238 were negative in all situations (Figure 2).

239 The most persistent compounds were acesulfame, 1H-benzotriazole, carbamazepine, 10,11-dihydro-
240 10,11-dihydroxy-carbamazepine and O-desmethylvenlafaxine, all of them showing median k_{att} > -0.01 h^{-1}
241 and <0.01 h^{-1} (IQR<0.04 h^{-1}) in all four situations (Table 1). Persistence of carbamazepine, acesulfame and
242 1H-benzotriazole was reported previously and carbamazepine and acesulfame were used as conservative
243 wastewater tracers in former studies.[12,18,33,38,55] Writer et al.[33] measured a k_{att} (±SE) of 0.033 ± 0.009 h^{-1} of
244 carbamazepine in Boulder Creek, Colorado, which is slightly above the IQRs of k_{att} distributions measured
245 in River Erpe (3rd Quartiles: 0.012-0.022 h^{-1}). Aymerich et al.[37] even found a slight increase in
246 carbamazepine concentration in a receiving river in Spain reporting a k_{att} (±SD) of -0.4 ± 0.7d^{-1}, equivalent
247 to -0.017 h^{-1}, which is lower than the IQRs of k_{att} distributions in River Erpe (1st Quartiles: -0.010 - -0.003
248 h^{-1}). In contrast, Acuña et al.[39] reported a carbamazepine half-life (±SD) of 4.1 ± 2.4 h measured as an
249 average of four rivers in Spain, which converts to a k_{att} of 0.17 h^{-1}, i.e. an order of magnitude higher than
250 the IQRs of k_{att} measured in the present study. This value is exceptional, also because many laboratory

studies found low degradation of carbamazepine. No decay of carbamazepine was observed in a 30-day river-simulating flume study.[38] Also in a river sediment batch experiment carbamazepine was not significantly removed within 30 days.[18]

Acesulfame was found relatively constant (-2.9-0.8% relative attenuation) in four different rivers in Europe,[38] which compares well to 0 - 3% attenuation in the present study. However, interestingly acesulfame persistence in WWTPs was found to have decreased within the last decade because acesulfame degrading bacteria have evolved in WWTPs.[56] This effect is also conceivable for bacterial communities in rivers and might lead to observations of higher acesulfame in-stream k_{att}s in the future.

Although the corrosion inhibitor 1H-benzotriazole shows high concentrations in WWTP effluents in Europe,[4] to the best of our knowledge its in-stream attenuation has not been studied prior to our study. However, poor removal has been found in laboratory studies and in bank filtration.[55,57]

Relative attenuation and half-lifes of all TrOCs are shown in Table S6. It has been reported previously, that passive samplers are a useful means to accompany in-stream attenuation studies and lead to similar results as obtained through high-resolution sampling.[38] A comparison of k_{att} for 11 (*bm*) and 10 days (*am*) obtained from passive samplers to median k_{att} in the 2-day sampling periods indicates the same trends between S1bm and S1am for 13 out of 17 compounds (Figure S6). Thus, differences in k_{att} attributed to macrophyte removal are not only a short-term phenomenon, but are also valid over an extended time period. A detailed discussion is provided in the SI.

Environmental conditions and implications for processes in the sampling situations

In order to allow appropriate interpretation of the results, the differences in environmental conditions and implications for attenuation processes between the sampling situations have to be taken into account. Photolysis of TrOCs (both direct and indirect) is expected to be mainly driven by diurnal fluctuations of solar radiation within sampling-periods, changes in intensity of solar radiation between

sampling periods and differences in shading between sections.[22,40] Biodegradation is more complex due to the variable nature of microbial communities and (co-) metabolic degradation processes.[58] However, the composition of communities is assumed to be relatively constant in diversity and in processing intensity due to the constantly high proportion of treated wastewater in the River Erpe. Hotspots of biodegradation occur mainly at ecohydrological interfaces, i.e. in biofilms at the surface of submerged macrophytes or in the hyporheic zone.[20] Hence, biodegradation is spatially variable, due to heterogeneous flow regimes and sediment properties and also temporally due to changing presence of macrophytes. In addition, microbial activity is sensitive to daily fluctuations in temperature as respiration and carbon consumption of microbial communities is closely related to temperature.[59,60] Similar to biodegradation, sorption is influenced by the availability of ecohydrological interfaces. Therefore, changes in macrophyte abundance and differences in hyporheic exchange might lead to differences in attenuation of TrOC sensitive to sorption processes, mainly compounds that are positively charged at the prevailing pH of 7.8.[24,33] A more detailed discussion about the distinct relations between conditions and processes can be found in the SI.

The experimental setup produced two spatial comparisons (S1am vs. S2am and S1bm vs. S2bm) and two temporal comparisons (S1am vs. S1bm and S2am vs. S2bm). The differences in attenuation between the sections are expected to have been governed by the aforementioned characteristics: the higher ratio of shading in S2 is expected to generally have impaired photolysis compared to S1, especially *am*, when the macrophytes were not providing additional shading to S1. The higher potential for transient storage, in turn, is generally expected to have promoted biodegradation and sorption, especially *bm* when macrophytes contributed to the transient storage zone and provided more ecohydrological interfaces in S1. The temporal comparison *am* vs. *bm* is governed by the removal of macrophytes in S1, but differences might also have been caused by higher solar radiation in the sampling period *am* compared to *bm*. The absence of macrophytes in S1am is expected to have reduced the potential for

biodegradation and sorption compared to S1bm due to minimizing the filter-effect of macrophytes. However, as a result of the reduction of in-channel shading, the potential for photolysis was likely increased comparing S1am to S1bm. The abundance of macrophytes was generally low in S2 and no external changes took place, so differences between S2bm and S2am were probably for the most part caused by higher solar radiation *am*. A summary of the comparisons of the distinct environmental conditions and their implication for the differences in attenuation processes in the four sampling situations is shown in Table 2. Differences in average (±SD) DOC (S1bm: 11.0 ± 0.9 mg L^{-1}; S1am: 12.1 ± 1.8 mg L^{-1}; S2bm: 11.3 ± 0.8 mg L^{-1}; S2am: 12.1 ± 1.5 mg L^{-1}),nutrient concentrations (e.g. Nitrate-N: S1bm: 7.3 ± 0.9 mg L^{-1}; S1am: 6.8 ± 0.6 mg L^{-1}; S2bm: 7.2 ± 0.8 mg L^{-1}; S2am: 6.9 ± 0.6 mg L^{-1}) and water temperature (S1bm: 18.5 ± 0.9 °C; S1am: 19.5 ± 1.4 °C; S2bm: 18.6 ± 0.9 °C; S2am: 19.9 ± 1.8 °C) between the sampling situations are low and the effects on fate of TrOCs are assumed to be negligible (Table S1).

Influence of diurnal fluctuations in solar radiation and water temperature on TrOC attenuation

Environmental conditions may not only have varied between the sampling situations, but also within the single sampling-periods. Some of the high distributions of k_{att} within single sampling situations (eg. 4-hydroxydiclofenac in S1am: IQR 0.30 h^{-1}) are expected to have been be caused by diurnal fluctuations in certain conditions. There were probably a multitude of parameters that controlled attenuation processes which varied within the two days of sampling and it remains challenging to capture the full picture. We chose to correlate solar radiation and water temperature to k_{att} as they are parameters that (1) are potentially strongly related to the fate of TrOCs, (2) vary considerably within hours and (3) were easy to record continuously and reliably. High, significant correlations ($\rho > 0.5$; $p < 0.05$) were found for solar radiation and k_{att} of 4-hydroxidiclofenac in S1am ($\rho = 0.66$; $p < 0.05$) and hydrochlorothiazide in S1am ($\rho = 0.63$; $p < 0.05$) and S2am ($\rho = 0.57$; $p < 0.05$) and for water temperature and k_{att} of metoprolol ($\rho = 0.63$; $p < 0.05$), tramadol ($\rho = 0.51$; $p < 0.05$), sitagliptin ($\rho = 0.59$; $p < 0.05$), venlafaxine ($\rho = 0.54$; $p <$

0.05) and guanylurea ($\rho = 0.51$; $p < 0.05$) in S1bm, as well as 4-hydroxydiclofenac ($\rho = 0.57$; $p < 0.05$) in S1am (Table 1, Figure 3).

Attenuation of single compounds

In this work only attenuation behaviour of compounds that exhibit significant differences between situations and related parent compounds or TPs are discussed in detail, since they are most relevant for identification of processes (Table 1). These compounds are allocated to three groups according to their attenuation (median k_{att}) behaviour (Figure 2, Table 2). Group 1 (4-hydroxydiclofenac, diclofenac, hydrochlorothiazide) shows highest attenuation and correlation to solar radiation in S1am, additionally higher median k_{att} in S2am compared to S2bm. Group 2 (metoprolol, metoprolol acid, valsartan, valsartan acid) shows highest attenuation or formation in S1bm and generally lower attenuation or formation in S2 than S1. Group 3 (metformin, guanylurea, bezafibrate) shows highest attenuation without high correlation to solar radiation in S1am and similar attenuation in the remaining situations. Sulfamethoxazole does not fit in either of the groups, but has been reported to be affected by both biodegradation and photolysis, including potential back-transformation.[61,62] The combination of processes might explain the high distribution of k_{att} of sulfamethoxazole in all situations and back-transformation might be responsible for net-formation in S2.

Group 1: Diclofenac and Hydrochlorothiazide

Diclofenac, its TP 4-hydroxydiclofenac and hydrochlorothiazide all behaved in a similar manner (Figure 2). Attenuation of all three compounds significantly increased in S1 following macrophyte removal and higher in S2am at higher average insolation, compared to S2bm. Both diclofenac and hydrochlorothiazide were previously reported to be highly photodegradable relative to other compounds.[16,37,40] The correlation of k_{att} in single water parcels with solar radiation confirms this. The highest observed ρ for correlation between solar radiation and k_{att} were found in S1am for diclofenac ($\rho = 0.49$; $p < 0.05$),

4-hydoxydiclofenac ($\rho = 0.66$; $p < 0.05$) and hydrochlorothiazide ($\rho = 0.63$; $p < 0.05$) and in S2am for hydrochlorothiazide ($\rho = 0.57$; $p < 0.05$) (Table 1).

While aerobic biodegradation of diclofenac has been reported and 4-hydroxydiclofenac was found to be its major oxidative biotransformation product,[18,63] several recent studies did not observe biotransformation.[15,16] The high correlation with solar radiation and the fact that 4-hydroxydiclofenac behaves similarly to its parent compound and mostly decreased along the reach suggests that still photolysis was the main degradation process in S1bm, S1am and S2am. In S2bm, where least penetration of the surface water by solar radiation is expected (Table 2), median k_{att} of 4-hydroxydiclofenac were clearly negative indicating formation. This suggests a higher influence of biotic transformation of diclofenac to 4-hydroxydiclofenac in S2bm. To the best of our knowledge, the only other study reporting in-stream fate of both compounds was conducted by Aymerich et al.[37] comparing attenuation rates of a WWTP and its receiving river. They found k_{att} (±SD) of 0.8 ± 0.9 d^{-1} (0.03 h^{-1}) for diclofenac and 4.4 ± 1.7 d^{-1} (0.18 h^{-1}) for 4-hydroxydiclofenac in a 4 km-reach which compare very well with the median k_{att} of 0.04 h^{-1} (IQR 0.08 h^{-1}) for diclofenac and 0.21 h^{-1} (IQR 0.30 h^{-1}) for 4-hydroxydiclofenac in S1am in the present study.

Hydrochlorothiazide was previously found to transform to chlorothiazide (among other TPs) even under abiotic, dark control conditions by hydrolysis.[17,18] Compared to abiotic transformation, microbial transformation of hydrochlorothiazide plays a minor role.[16,18] Nevertheless, hydrolysis and biotransformation are expected to be of little importance compared to photolysis of hydrochlorothiazide. A river-simulating flume study under dark conditions resulted in a k_{att} of 0.0005 h^{-1} of hydrochlorothiazide, which is up to two orders of magnitude lower than the rate constants in the present study.[17] In addition the high correlation of hydrochlorothiazide with solar radiation in all four situations shows the prevalence of photolysis as major degradation process. In contrast to diclofenac and its TP, the behaviour of chlorothiazide does not resemble the attenuation of hydrochlorothiazide and

might be a result of more complex transitions of processes. This is in agreement with the suggestion that chlorothiazide is likely an intermediate in the transformation sequence of hydrochlorothiazide and other TPs.[38,63]

The findings for group 1 compounds show that their attenuation was governed by photolysis and their attenuation pattern is in accordance with the expectations for photolysis in Table 2. Interestingly, in S1am all three compounds show significant correlation (ρ = 0.44, 0.52, 0.45 and 0.33 respectively; $p < 0.05$) with water temperature as well, which may be explained by the fact that quantum yield, and thus photolysis rate increases with water temperature.[64] The high correlation of hydrochlorothiazide attenuation with solar radiation (Figure 3) makes it a potential future candidate for tracing intrinsic photolytical processes in contaminated rivers.

Group 2: Metoprolol and Valsartan

Metoprolol and valsartan show behaviour similar to each other. Despite higher solar radiation and higher water temperature in S1am compared to S1bm, their attenuation was highest in S1bm (significantly in the case of metoprolol) indicating the prevailing role of macrophytes. Their attenuation is generally higher in S1 compared to S2 and in S2 attenuation does not differ considerably *bm* compared to *am* (Figure 2). In several previous studies valsartan and metoprolol were found to be biodegradable.[18,19,36,63,65]

The β-blocker metoprolol is not sensitive to photolysis.[16] It is mostly cationic at ambient pH of 7.8, potentially facilitating sorption via electrostatic interactions to negatively charged surfaces. Both processes can be promoted by hyporheic exchange and by high abundance of biofilm and are normally hard to distinguish in the field.[17-19] Hence, it is conceivable that the higher attenuation in S1 compared to S2 is caused by biodegradation and/or sorption. However, during presence of macrophytes in S1bm where particularly high attenuation was found, a strong correlation of k_{att} to water temperature was

391 observed. Since sorption is commonly inversely correlated with temperature, it is likely not the main
392 removal process in this situation.[66,67] In addition, other positively charged compounds (metformin,
393 guanylurea, tramadol, soatalol, sitagliptin, except for venlafaxine) show comparably low median k_{att}
394 (<0.01 h^{-1}; IQR<0.06 h^{-1}) in S1bm and higher median k_{att} in S1am. This indicates that higher abundance of
395 epiphytic biofilm and thus negatively charged binding sites did generally not increase the attenuation of
396 positively charged compounds. We can conclude that in S1bm biodegradation is most likely the
397 governing process for increased metoprolol attenuation caused by the presence of macrophytes. We
398 suspect that epiphytic biofilms are mainly responsible for the degradation and the correlation of
399 degradation with temperature of metoprolol in S1bm. The fact that even after removal of macrophytes,
400 degradation was higher in S1 compared to S2 indicates that a generally larger transient storage zone in
401 S1 contributes to higher attenuation by biodegradation or sorption of metoprolol considerably. In a
402 flume-experiment without macrophytes conducted by Li et al.[17] an average k_{att} of 0.005 h^{-1} was measured
403 for metoprolol, which is very close to the median k_{att} of 0.006 h^{-1} (IQR 0.03 h^{-1}) found in the present study
404 in S2bm.

405 Its TP metoprolol acid is a biotransformation product[65] and shows a net-negative median k_{att}, i.e. net-
406 formation. “Mirroring” the degradation of metoprolol, median formation was highest in S1bm and
407 lowest in S2bm. However, metoprolol acid is not only formed by metoprolol transformation, but also
408 derives from e.g. atenolol degradation.[68] Despite metoprolol acid being the major TP of metoprolol,
409 metoprolol transforms into a set of other TPs as well.[69] That is why despite the resemblance no mass
410 balance between metoprolol degradation and metoprolol acid formation is possible. In contrast to
411 metoprolol, no significant relation of metoprolol acid formation to water temperature was observed.
412 This suggests that formation in the hyporheic zone, which has been reported earlier,[17] may be of higher
413 importance than epiphytic biofilm. Due to temperature dampening, the correlation of water
414 temperature and biodegradation is expected to be less pronounced in the hyporheic zone compared to

415 the surface water.[70] For the second TP of metoprolol, α-hydroxymetoprolol, attenuation overweighs
416 formation. No significant differences between situations and no significant correlations to temperature
417 or radiation were found, indicating that attenuation pathways are more complex than for metoprolol.
418 Batch experiments indicated that α-hydroxymetoprolol is less persistent than metoprolol acid.[63,69] In
419 addition, in a field study comparing TrOC fate in four rivers, formation of metoprolol acid was observed
420 in two rivers, while attenuation of α-hydroxymetoprolol was found in all four rivers. Thess findings are in
421 line with the observation of the present study.

422 Valsartan did not undergo abiotic transformation or sorption to sludge in batch experiments, neither has
423 it been reported to undergo photolysis.[68,71] Despite its resemblance in behaviour to metoprolol, its k_{att}
424 did not correlate to water temperature and did not differ significantly *bm* and *am*. However, its
425 attenuation was generally higher in S1 than S2, which can be attributed to biodegradation enhanced by
426 the larger transient storage zone in S1. Noedler et al. [71] showed that valsartan biodegradation increased
427 in solutions with higher effluent portion. In contrast metoprolol biodegradation decreased with higher
428 effluent portion. This confirms the idea, that valsartan might be degraded by a different community (e.g.
429 sediment) than metoprolol (e.g. epiphytic biofilm). Despite its high relevance (valsartan concentrations
430 were six times higher than metoprolol concentrations), in-stream fate of valsartan has been rarely
431 studied. Only Acuña et al.[39] measured valsartan concentrations in four different rivers and found average
432 k_{att} of 0.32 h^{-1}, which is an order of magnitude higher than the k_{att} observed in the present study (Table
433 1). The authors found that the process of valsartan removal is linked to phosphorous dynamics.
434 However, no correlation to phosphorous attenuation was found in the present study (data not shown).

435 Similar to metoprolol acid, valsartan acid resembles the degradation of its parent compound in its
436 formation patterns (Figure 2). Higher formation was observed in S1 than S2, no temperature-
437 dependence was found and removal of macrophytes did not impact the formation, indicating again
438 biotransformation in the hyporheic zone. However, the compound has a set of other parent compounds

439 in the sartan-group[12] (e.g. irbesartan) and the transformation sequence deriving from valsartan has at
440 least two intermediates[68]. Therefore, relation between attenuation of valsartan and formation of
441 valsartan acid remains speculative. While metoprolol acid was reported to show limited persistence,[63,65]
442 valsartan acid was found to be more persistent[12,65]. In our experiment, formation of both compounds
443 was generally in the same order of magnitude, indicating that the residence time was too short for an
444 onset of metoprolol acid degradation, and further formation of valsartan acid at longer travel times is
445 conceivable. The environmental relevance of valsartan acid due to its high concentrations, potential
446 formation in ecosystems and high persistence has been highlighted earlier.[12,65,68] However, to the best of
447 our knowledge, this is the first time in-stream formation of valsartan acid was described and studied in
448 situ. The findings for group 2 compounds show that their attenuation and formation were governed by
449 biodegradation and their behaviour is in accordance with the expectations for biodegradation in Table 2.

450 *Group 3: Metformin and Bezafibrate*

451 Metformin and its biodegradation product guanylurea show generally low attenuation under the studied
452 conditions. Trautwein et al.[72] tested aerobic transformation of both compounds and concluded that most
453 of the transformation from metformin to guanylurea is likely happening in the WWTP and is unlikely in
454 the aquatic environment. Due to the high concentration of guanylurea compared to metformin at station
455 A (approx. 40:1, Table 1), our study confirms high transformation prior to discharge into River Erpe. Also
456 the observed median k_{att} of both compounds are in the range of those of carbamazepine (<0.01 h^{-1}) and
457 are therefore relatively persistent in S1bm, S2bm and S2am. However, for both compounds higher
458 attenuation was found in S1am, significantly for guanylurea. In contrast to diclofenac and
459 hydrochlorothiazide, their attenuation is not related to solar radiation and studies show that photolysis
460 does not affect their fate in surface waters.[72] Guanylurea is expected to be a dead-end bio-TP and even
461 breakdown by ozone is limited.[73] Both compounds are positively charged under ambient pH and
462 electrostatic binding to negatively charged soil particles was reported previously.[74] Hence, sorption could

be a reason for the increased attenuation in S1am. A possible explanation is a higher contact to specific binding sites caused by disruption of the upper sediment layer by the mowing machines. Bezafibrate again shows similar behaviour but is negatively charged. It was found to show abiotic hydrolytic reaction and biotransformation previously.[17,65] The distinct processes causing the attenuation pattern of group 3 remain a subject of speculation and might be of different nature for bezafibrate and metformin/guanylurea. Little research has been done on the environmental fate of guanylurea so far, despite its particular high concentrations and unknown toxicity.[46] Further studies are needed to elucidate its degradation behaviour.

General within-stream variability

The methods applied in the present studies are associated with different uncertainties inherent in field experiments and only a selection of possible environmental drivers for the fate of TrOC could be studied. A discussion about limitations can be found in the SI. Nevertheless, the present study shows that spatially different and temporally changing conditions within a river influence attenuation processes. They result in a range of river-specific k_{att} values rather than single values. Although the behaviour of TrOCs was compound-specific, some general statements about the differences between sections, the effect of macrophyte removal and the influence of diurnal changes are possible.

a) A clear difference between sections was found. Shading by canopy in S2 was seen to clearly reduce breakdown of photosensitive compounds (group 1) compared to S1am. The effect of shading by submerged macrophytes in S1bm showed similar (hydrochlorothiazide) or lower effect (diclofenac) than shading by the canopy in S2bm. Higher potential for transient storage in S1 lead to higher attenuation/formation of the biodegradable/bioformable compounds (group 2) in S1 compared to S2 both *bm* and *am*.

b) Macrophyte removal had different effects: The decreased macrophyte-induced shading of the channel increased the photolysis of photosensitive compounds. At the same time, it

decreased the attenuation of metoprolol significantly, which has likely occurred on epiphytic biofilm. Other compounds exhibited high correlation of k_{att} with water temperature in S1bm even at low k_{att} values (guanylurea, sitagliptin, tramadol, venlafaxine) (Table 1). This leads to the assumption that the presence of macrophytes generally promoted the influence of temperature on biodegradation. The impact of macrophytes on drivers of TrOC attenuation is highlighted by the fact, that high correlation with solar radiation is primarily seen in S1am and high correlation with water temperature, in contrast, mostly in S1bm.

c) Diurnal changes of solar radiation have significant influence on the breakdown of photosensitive compounds, especially in the situation of least shading (S1am). Water temperature influences particularly attenuation of metoprolol in the situation of high macrophyte density (S1bm).

In-stream fates of some compounds of high environmental concern, e.g. guanylurea, 1H-benzotriazole and valsartan acid were reported for the first time. Further studies on their environmental fate are of great importance. Some of the variations in TrOC attenuation of River Erpe could be explained by changes in environmental conditions and lead to identification of situation-dependent attenuation processes. Therefore, we want to emphasize within-stream attenuation studies as opposed to between-streams studies as a valuable means to better identify transformation processes. Eventually better understanding of in-stream attenuation processes of TrOCs will improve the predictability of their environmental fate and benefit both, regulatory decision making and river management.

Acknowledgements

The work has received funding from the European Union's Horizon 2020 research and innovation programme under Marie Sklodowska-Curie grant agreement No 641939 and additionally from the Research Training Group 'Urban Water Interfaces (UWI)' (GRK 2032/1) funded by the German Research

Foundation (DFG). We thank the three anonymous reviewers and the editor for their helpful comments. The Berlin Water Works and the WWTP facility Münchehofe are gratefully acknowledged for providing information. We also thank Anne Mehrtens, Wiebke Seher, Karin Meinikmann, Margaret Shanafield and Christine Sturm for their support in the field. In addition we thank Jason Galloway, Jon Benskin, Juliane Hollender, Mario Schirmer, Anna Sobek and Stefan Krause for their contribution and supervision.

Supporting Information

Background data; deconvolution method; concentration curves of slelected TrOCs; discussions on relation of attenuation processes to environmental conditions; passive sampler methods and results; details on k_{att} distributions.

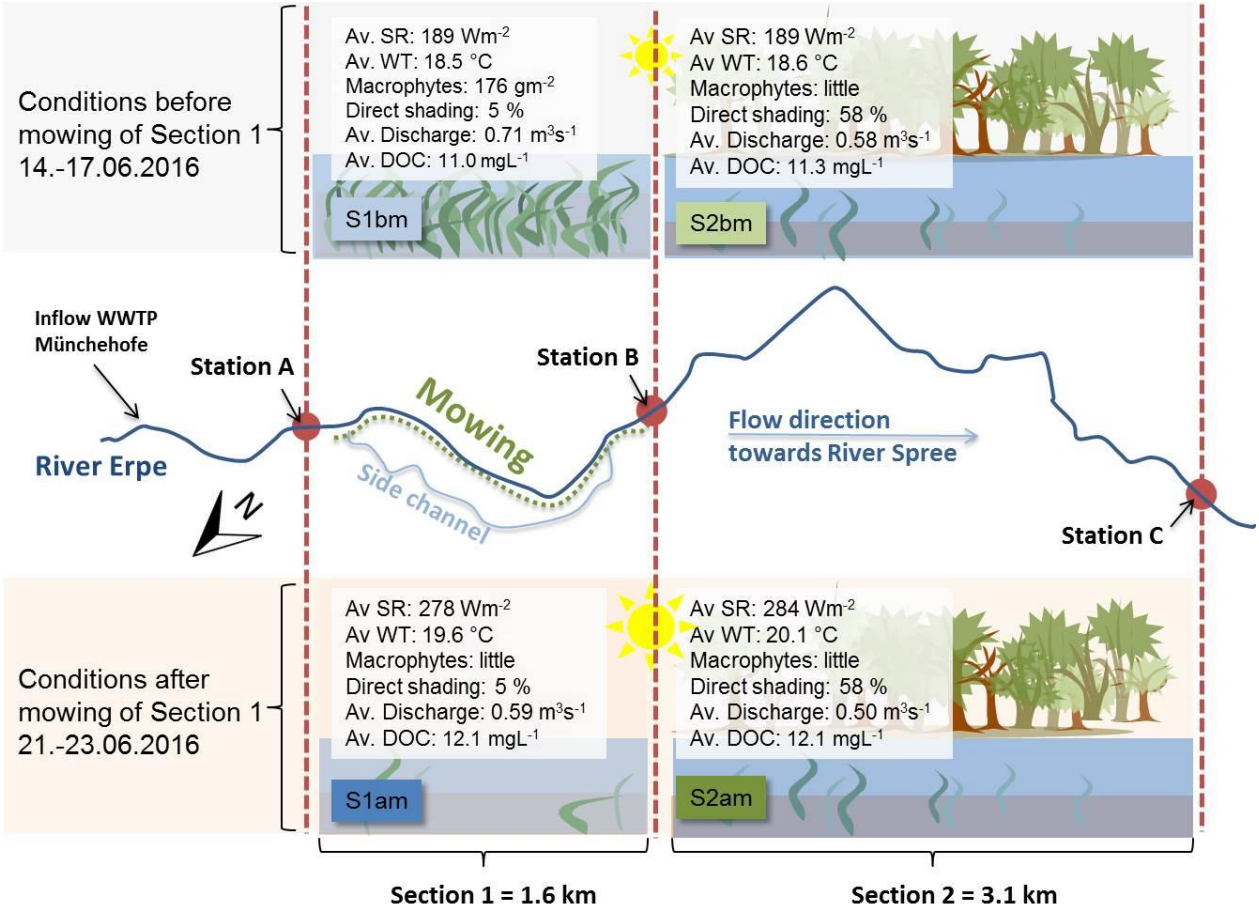

Figure 1 Map of the 4.7 km study reach of River Erpe, located in the east of Berlin, Germany. The three sampling stations A, B and C, downstream of the WWTP inflow, determine the two study sections 1 and 2. The mowing area is shown in a green-dashed line. Graphics below and above depict comparison of attenuation conditions between sections and before and after mowing of section 1. Av. SR= average solar radiation; Av. WT= average water temperature; Av. DOC= average dissolved organic carbon.

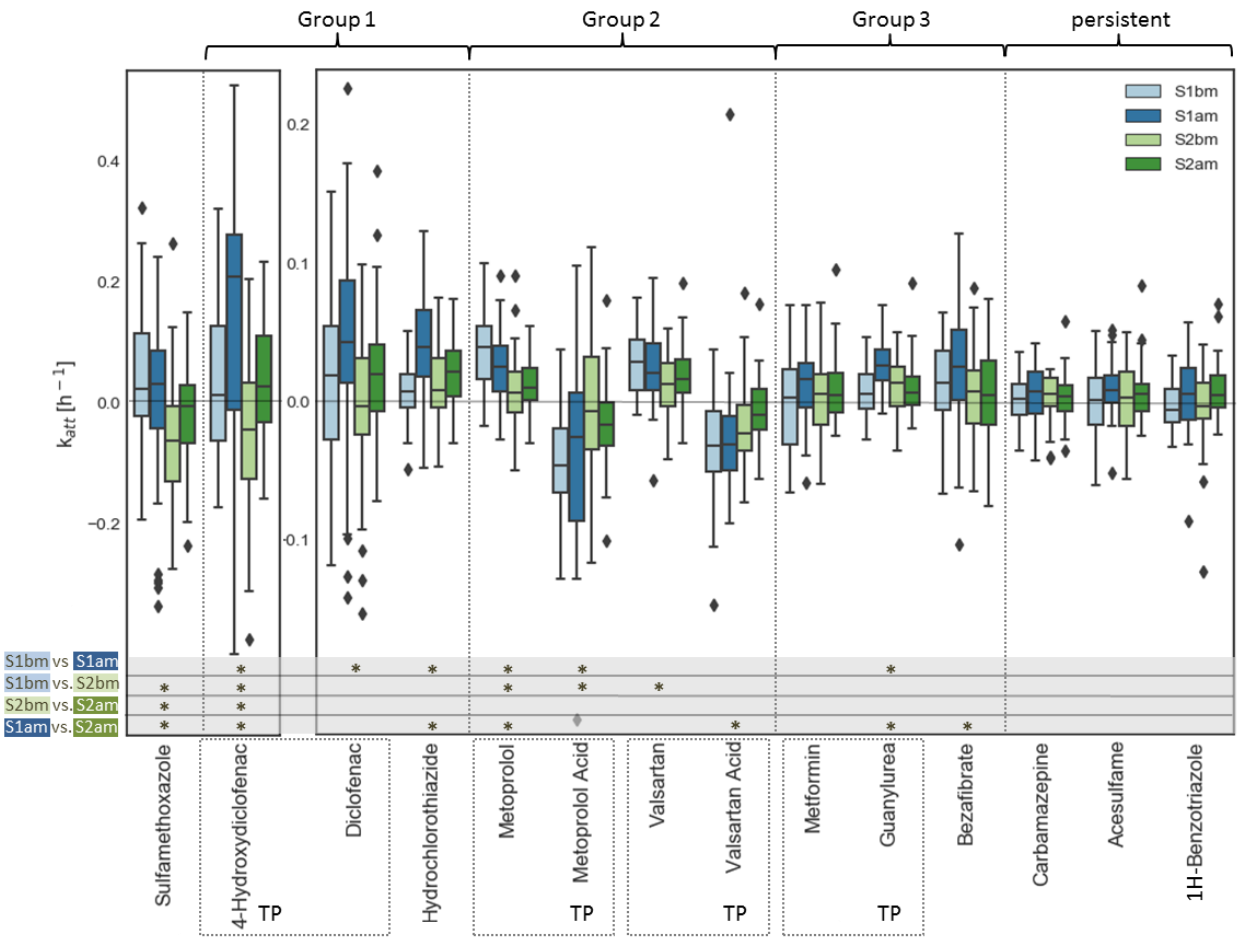

532

533 **Figure 2** Distributions of attenuation rate constants (k_{att}) of all compounds in the different sampling situations that showed
534 significant differences between sampling situations as well as metformin, carbamazepine, acesulfame and 1H-benzotriazole for
535 comparison. Boxes indicate quartiles, while whiskers show the rest of the distribution without outliers and diamonds represent
536 outliers. S1bm: n=48; S1am: n=47; S2bm: n=47; S2am: n=46. The bottom four lines show significant differences between
537 sampling situations in Conover tests (*: $p<0.05$). Dashed boxes indicate pairs of parent compounds and TPs. Compounds were
538 allocated to the groups according to their attenuation patterns.

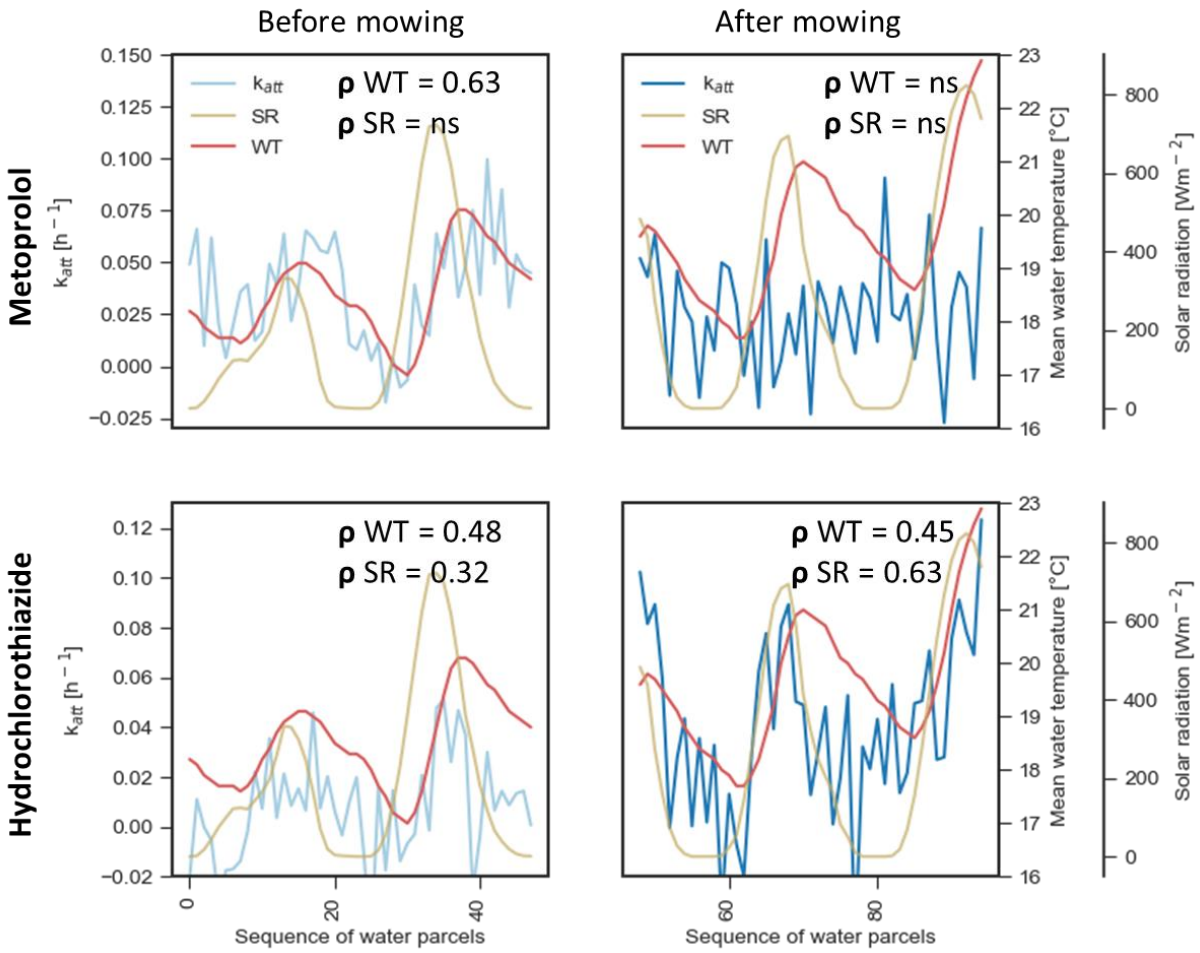

539

540 **Figure 3** Exemplary fluctuation in attenuation rate constants (k_{att}), average water temperature (WT), and average solar radiation
541 (SR) in the hourly sequence of 48 water parcels S1bm (starting 14.06.2016 23:00) and 47 water parcels S1am (starting
542 21.06.2016 18:00), respectively comparing the compounds metoprolol and hydrochlorothiazide. ρ WT = Spearman correlation
543 coefficient between k_{att} and average water temperature; ρ SR = Spearman correlation coefficient between k_{att} and average solar
544 radiation. ns = no significant correlation.

545 .

Table 1 List of compounds with average concentrations and loads at station A, median attenuation rate constant k_{att}, Kruskal-Wallis test and Conover test results and Spearman correlation values. ns = no significant correlation. Details on the statistics are shown in Table S2, half-lives and relative attenuation in Table S6 and k_{att} uncertainties in Table S9.

Compound (parent compounds are highlighted in bold, related TPs are listed below)	Average concentrations st. A (max, min) [µg L^{-1}]	Av. loads st. A [g day^{-1}]	Median k_{att} [h^{-1}]				Kruskal-Wallis test (KW) and Post-hoc test: Conover with Benjamini, Krieger and Yekutieli correction * $p < 0.05$					Spearman correlation coefficient ρ							
												Solar radiation vs. k_{att}				Water temperature vs. k_{att}			
			S1bm n=48	S1am n=47	S2bm n=47	S2am n=46	KW	S1bm vs S1am	S1bm vs S2bm	S2bm vs S2am	S1am vs S2am	S1-bm	S1-am	S2-bm	S2-am	S1-bm	S1-am	S2-bm	S2-am
Acesulfame	2.90 (4.9, 1.4)	174	0.0010	0.0082	0.0027	0.0061	ns					ns	-0.31	0.33	ns	0.41	-0.32	ns	ns
1H-Benzotriazole	10.7 (18, 5.5)	633	(-0.0057)	0.0059	(-0.0031)	0.0051	*	ns	ns	ns	ns	ns	ns	0.41	ns	0.31	ns	ns	ns
Bezafibrate	0.564 (0.88, 0.37)	34	0.0141	0.0251	0.0071	0.0045	*	ns	ns	ns	*	ns	ns	0.36	ns	0.37	ns	ns	ns
Carbamazepine	1.53 (1.9, 1.0)	91	0.0021	0.0074	0.0060	0.0035	ns					ns	ns	ns	ns	0.48	ns	ns	ns
10,11-Dihydro-10,11-dihydroxy Carbamazepine	2.84 (4.1, 1.7)	168	0.0033	0.0064	0.0085	0.0013	ns					ns	ns	ns	ns	ns	ns	ns	ns
Carbamazepine-10,11-Epoxide	0.063 (0.11, 0.029)	4	0.0113	0.0097	(-0.0028)	0.0190	ns					ns	ns	ns	ns	ns	ns	0.31	ns
Diclofenac	3.36 (5.0, 1.7)	199	0.0190	0.0428	(-0.0031)	0.0198	*	*	ns	ns	ns	ns	0.49	0.41	ns	0.34	0.44	ns	ns
4-Hydroxydiclofenac	0.585 (1.5, 0.13)	34	0.0134	0.2102	(-0.0427)	0.0291	*	*	*	*	*	0.30	0.66	ns	ns	ns	0.57	-0.31	-0.43
Hydrochlorothiazide	5.68 (7.6, 3.4)	338	0.0074	0.0393	0.0079	0.0214	*	*	ns	ns	*	0.32	0.63	0.36	0.57	0.48	0.45	ns	0.33
Chlorothiazide	0.173 (0.24, 0.078)	10	(-0.0162)	(-0.0089)	0.0179	(-0.0005)	ns					ns	ns	ns	ns	ns	ns	ns	ns
Irbesartan	1.74 (2.3, 0.96)	103	(-0.0063)	0.0109	(-0.0014)	0.0094	ns					ns	ns	ns	ns	0.45	ns	-0.36	ns
Metformin	1.74 (4.39, 1.73)	105	0.0028	0.0162	0.0052	0.0052	ns					ns	ns	0.36	ns	ns	ns	ns	-0.36
Guanylurea	68.8 (90, 46)	4107	0.0058	0.0263	0.0137	0.0067	*	*	ns	ns	*	ns	ns	ns	-0.39	0.51	ns	ns	ns
Metoprolol	4.40 (5.9, 2.1)	262	0.0392	0.0256	0.0062	0.0105	*	*	*	ns	*	ns	ns	ns	ns	0.63	ns	ns	ns
α-Hydroxy-Metoprolol	0.503 (0.73, 0.31)	30	0.0330	0.0464	0.0272	0.0238	ns					ns	ns	ns	ns	ns	ns	ns	ns
Metoprolol Acid	0.245 (0.41, 0.10)	14	(-0.0461)	(-0.0253)	(-0.0072)	(-0.0170)	*	*	*	ns	ns	ns	ns	ns	ns	ns	ns	ns	ns
Sitagliptin	3.57 (4.5, 1.9)	213	0.0059	0.0151	0.0159	0.0037	ns					ns	ns	ns	ns	0.59	ns	ns	ns
Sotalol	0.221 (0.29, 0.13)	13	(-0.0059)	0.0183	0.0050	0.0068	ns					ns	ns	ns	ns	0.33	ns	ns	0.34
Sulfamethoxazole	0.066 (0.14, 0.018)	4	0.0248	0.0313	(-0.0613)	(-0.0035)	*	ns	*	*	*	ns	ns	ns	-0.39	ns	ns	ns	ns
Tramadol	0.847 (1.0, 0.50)	50	(-0.0006)	0.0129	0.0029	0.0045	ns					ns	ns	ns	-0.32	0.51	ns	ns	ns
Valsartan	28.5 (38, 17)	1693	0.0289	0.0206	0.0130	0.0161	*	ns	*	ns	ns	ns	ns	ns	ns	ns	ns	ns	ns
Valsartan Acid	5.41 (8.3, 2.4)	319	(-0.0319)	(-0.0307)	(-0.0211)	(-0.0091)	*	ns	ns	ns	*	ns	ns	ns	-0.41	ns	ns	ns	ns
Venlafaxine	0.325 (0.46, 0.16)	19	0.0102	0.0046	-0.0003	0.0057	ns					ns	ns	ns	ns	0.54	ns	ns	0.30
O-Desmethylvenlafaxine	1.58 (2.0, 0.95)	94	0.0050	0.0077	-0.0004	0.0019	ns					ns	ns	ns	-0.31	0.47	ns	ns	ns

548 **Table 2** Qualitative implications for biodegradation, photolysis and sorption comparing the specific, different spatial and
549 temporal conditions in the four sampling situations. S1bm vs S2bm means a spatial comparison under pristine macrophyte
550 abundance. S1bm vs. S1am means a temporal comparison, including the effect of macrophyte removal. S2bm vs S2am
551 means a temporal comparison without change in macrophyte abundance in section 2 but differences in solar radiation and
552 water temperature. S1am vs. S2am means a spatial comparison after macrophyte removal. For comparison the behaviour
553 of groups of compounds is added below (Group 1 = 4-hydroxydiclofenac, diclofenac, hydrochlorothiazide; Group 2 =
554 metoprolol, metoprolol acid, valsartan, valsartan acid; Group 3 = metformin, guanylurea, bezafibrate)

	S1bm vs. S1am	**S1bm vs. S2bm**	**S2bm vs. S2am**	**S1am vs. S2am**
Implications for Biodegradation	**Higher in S1bm** due to the biofilm on macrophytes and potential pumping effect, inducing higher hyporheic flow. However, water temperature was 1 °C lower than S1am.	**Higher in S1bm** due to higher abundance of macrophytes and better conditions for transient storage	**Slightly higher in S2am** due to higher water temperature	**Slightly higher in S1am** due to higher potential for transient storage
Implications for Photolysis	**Higher S1am**, due to deeper penetration of the radiation without macrophytes and 47 % higher solar radiation.	**Low in both cases**, due to in-channel shading by macrophytes in S1 and shading by tree canopies in S2	**Higher S2am**, due to higher solar radiation	**Higher S1am**, due to less shading by canopy
Implications for Sorption	**Higher in S1bm** due to the biofilm on macrophytes and potential pumping effect, inducing higher hyporheic flow.	**Higher in S1bm** due to higher abundance of macrophytes and better conditions for transient storage	**Similar**	**Slightly higher in S1am** due to higher potential for transient storage
Behaviour of Group 1	Median k_{att} **higher in S1am**	Median k_{att} **higher in S1bm or similar**	Median k_{att} **higher in S2am**	Median k_{att} **higher in S1am**
Behaviour of Group 2	Absolute value of median k_{att} **higher in S1bm**	Absolute value of median k_{att} **higher in S1bm**	Absolute value of median k_{att} **mostly slightly higher in S2am**	Absolute value of median k_{att} **higher in S1am**
Behaviour of Group 3	Median k_{att} **higher in S1am**	Median k_{att} **similar**	Median k_{att} **similar**	Median k_{att} **higher in S1am**

(1) Reemtsma, T.; Berger, U.; Arp, H. P. H.; Gallard, H.; Knepper, T. P.; Neumann, M.; Quintana, J. B.; Voogt, P. d., Mind the Gap: Persistent and Mobile Organic Compounds—Water Contaminants That Slip Through. *Environ. Sci. Technol.* **2016,** *50*, (19), 10308-10315.
(2) Daughton, C. G.; Ternes, T. A., Pharmaceuticals and personal care products in the environment: agents of subtle change? *Environmental Health Perspectives* **1999,** *107*, (Suppl 6), 907-938.
(3) Farré, M. l.; Pérez, S.; Kantiani, L.; Barceló, D., Fate and toxicity of emerging pollutants, their metabolites and transformation products in the aquatic environment. *TrAC Trends in Analytical Chemistry* **2008,** *27*, (11), 991-1007.
(4) Loos, R.; Carvalho, R.; António, D. C.; Comero, S.; Locoro, G.; Tavazzi, S.; Paracchini, B.; Ghiani, M.; Lettieri, T.; Blaha, L.; Jarosova, B.; Voorspoels, S.; Servaes, K.; Haglund, P.; Fick, J.; Lindberg, R. H.; Schwesig, D.; Gawlik, B. M., EU-wide monitoring survey on emerging polar organic contaminants in wastewater treatment plant effluents. *Water Research* **2013,** *47*, (17), 6475-6487.
(5) Verlicchi, P.; Al Aukidy, M.; Zambello, E., Occurrence of pharmaceutical compounds in urban wastewater: Removal, mass load and environmental risk after a secondary treatment—A review. *Sci. Total Environ.* **2012,** *429*, 123-155.
(6) Thomaidi, V. S.; Stasinakis, A. S.; Borova, V. L.; Thomaidis, N. S., Is there a risk for the aquatic environment due to the existence of emerging organic contaminants in treated domestic wastewater? Greece as a case-study. *Journal of Hazardous Materials* **2015,** *283*, 740-747.
(7) Jekel, M.; Ruhl, A. S.; Meinel, F.; Zietzschmann, F.; Lima, S. P.; Baur, N.; Wenzel, M.; Gnirß, R.; Sperlich, A.; Dünnbier, U.; Böckelmann, U.; Hummelt, D.; van Baar, P.; Wode, F.; Petersohn, D.; Grummt, T.; Eckhardt, A.; Schulz, W.; Heermann, A.; Reemtsma, T.; Seiwert, B.; Schlittenbauer, L.; Lesjean, B.; Miehe, U.; Remy, C.; Stapf, M.; Mutz, D., Anthropogenic organic micro-pollutants and pathogens in the urban water cycle: assessment, barriers and risk communication (ASKURIS). *Environmental Sciences Europe* **2013,** *25*, (1), 1-8.
(8) Tröger, R.; Klöckner, P.; Ahrens, L.; Wiberg, K., Micropollutants in drinking water from source to tap - Method development and application of a multiresidue screening method. *Sci. Total Environ.* **2018,** *627*, 1404-1432.
(9) Loos, R.; Locoro, G.; Comero, S.; Contini, S.; Schwesig, D.; Werres, F.; Balsaa, P.; Gans, O.; Weiss, S.; Blaha, L.; Bolchi, M.; Gawlik, B. M., Pan-European survey on the occurrence of selected polar organic persistent pollutants in ground water. *Water Res* **2010,** *44*, (14), 4115-26.
(10) Ebele, A. J.; Abou-Elwafa Abdallah, M.; Harrad, S., Pharmaceuticals and personal care products (PPCPs) in the freshwater aquatic environment. *Emerging Contaminants* **2017,** *3*, (1), 1-16.
(11) Calvo-Flores, F. G.; Isac-Garcia, J.; Dobado, J. A., Regulations and Normatives. In *Emerging Pollutants: Origin, Structure, and Properties*, Wiley: 2017; pp 11-13.
(12) Nodler, K.; Hillebrand, O.; Idzik, K.; Strathmann, M.; Schiperski, F.; Zirlewagen, J.; Licha, T., Occurrence and fate of the angiotensin II receptor antagonist transformation product valsartan acid in the water cycle--a comparative study with selected beta-blockers and the persistent anthropogenic wastewater indicators carbamazepine and acesulfame. *Water Res* **2013,** *47*, (17), 6650-9.
(13) Banzhaf, S.; Nodler, K.; Licha, T.; Krein, A.; Scheytt, T., Redox-sensitivity and mobility of selected pharmaceutical compounds in a low flow column experiment. *Sci. Total Environ.* **2012,** *438*, 113-121.
(14) Barbieri, M.; Licha, T.; Nodler, K.; Carrera, J.; Ayora, C.; Sanchez-Vila, X., Fate of beta-blockers in aquifer material under nitrate reducing conditions: Batch experiments. *Chemosphere* **2012,** *89*, (11), 1272-1277.
(15) Schmidt, N.; Page, D.; Tiehm, A., Biodegradation of pharmaceuticals and endocrine disruptors with oxygen, nitrate, manganese (IV), iron (III) and sulfate as electron acceptors. *J. Contam. Hydrol.* **2017,** *203*, 62-69.
(16) Baena-Nogueras, R. M.; González-Mazo, E.; Lara-Martín, P. A., Degradation kinetics of pharmaceuticals and personal care products in surface waters: photolysis vs biodegradation. *Sci. Total Environ.* **2017,** *590-591*, 643-654.

(17) Li, Z.; Sobek, A.; Radke, M., Flume Experiments To Investigate the Environmental Fate of Pharmaceuticals and Their Transformation Products in Streams. *Environ. Sci. Technol.* **2015,** *49*, (10), 6009-6017.
(18) Radke, M.; Maier, M. P., Lessons learned from water/sediment-testing of pharmaceuticals. *Water Research* **2014,** *55*, 63-73.
(19) Velázquez, Y. F.; Nacheva, P. M., Biodegradability of fluoxetine, mefenamic acid, and metoprolol using different microbial consortiums. *Environmental Science and Pollution Research* **2017,** *24*, (7), 6779-6793.
(20) Krause, S.; Lewandowski, J.; Grimm, N. B.; Hannah, D. M.; Pinay, G.; McDonald, K.; Martí, E.; Argerich, A.; Pfister, L.; Klaus, J.; Battin, T.; Larned, S. T.; Schelker, J.; Fleckenstein, J.; Schmidt, C.; Rivett, M. O.; Watts, G.; Sabater, F.; Sorolla, A.; Turk, V., Ecohydrological interfaces as hot spots of ecosystem processes. *Water Resources Research* **2017,** *53*, (8), 6359-6376.
(21) Daneshvar, A.; Svanfelt, J.; Kronberg, L.; Prévost, M.; Weyhenmeyer, G. A., Seasonal variations in the occurrence and fate of basic and neutral pharmaceuticals in a Swedish river–lake system. *Chemosphere* **2010,** *80*, (3), 301-309.
(22) Schwarzenbach, R. P.; Gschwend, P. M.; Imboden, D. M., Direct Photolysis. In *Environmental Organic Chemistry*, John Wiley & Sons, Inc.: 2005; pp 611-654.
(23) Schwarzenbach, R. P.; Gschwend, P. M.; Imboden, D. M., Indirect Photolysis: Reactions with Photooxidants in Natural Waters and in the Atmosphere. In *Environmental Organic Chemistry*, John Wiley & Sons, Inc.: 2005; pp 655-686.
(24) Tülp, H. C.; Fenner, K.; Schwarzenbach, R. P.; Goss, K.-U., pH-Dependent Sorption of Acidic Organic Chemicals to Soil Organic Matter. *Environ. Sci. Technol.* **2009,** *43*, (24), 9189-9195.
(25) Torresi, E.; Polesel, F.; Bester, K.; Christensson, M.; Smets, B. F.; Trapp, S.; Andersen, H. R.; Plósz, B. G., Diffusion and sorption of organic micropollutants in biofilms with varying thicknesses. *Water Research* **2017,** *123*, 388-400.
(26) Kurz, M. J.; Drummond, J. D.; Marti, E.; Zarnetske, J. P.; Lee-Cullin, J.; Klaar, M. J.; Folegot, S.; Keller, T.; Ward, A. S.; Fleckenstein, J. H.; Datry, T.; Hannah, D. M.; Krause, S., Impacts of water level on metabolism and transient storage in vegetated lowland rivers: Insights from a mesocosm study. *J. Geophys. Res.-Biogeosci.* **2017,** *122*, (3), 628-644.
(27) Bohrman, K. J.; Strauss, E. A., Macrophyte-driven transient storage and phosphorus uptake in a western Wisconsin stream. *Hydrological Processes* **2018,** *32*, (2), 253-263.
(28) Boerema, A.; Schoelynck, J.; Bal, K.; Vrebos, D.; Jacobs, S.; Staes, J.; Meire, P., Economic valuation of ecosystem services, a case study for aquatic vegetation removal in the Nete catchment (Belgium). *Ecosystem Services* **2014,** *7*, 46-56.
(29) Miliša, M.; Kepčija, R. M.; Radanović, I.; Ostojić, A.; Habdija, I., The impact of aquatic macrophyte (Salix sp. and Cladium mariscus (L.) Pohl.) removal on habitat conditions and macroinvertebrates of tufa barriers (Plitvice Lakes, Croatia). *Hydrobiologia* **2006,** *573*, (1), 183-197.
(30) Matamoros, V.; Nguyen, L. X.; Arias, C. A.; Salvadó, V.; Brix, H., Evaluation of aquatic plants for removing polar microcontaminants: A microcosm experiment. *Chemosphere* **2012,** *88*, (10), 1257-1264.
(31) Gumbricht, T., Nutrient removal capacity in submersed macrophyte pond systems in a temperature climate. *Ecological Engineering* **1993,** *2*, (1), 49-61.
(32) Kunkel, U.; Radke, M., Reactive Tracer Test To Evaluate the Fate of Pharmaceuticals in Rivers. *Environ. Sci. Technol.* **2011,** *45*, (15), 6296-6302.
(33) Writer, J. H.; Antweiler, R. C.; Ferrer, I.; Ryan, J. N.; Thurman, E. M., In-Stream Attenuation of Neuro-Active Pharmaceuticals and Their Metabolites. *Environ. Sci. Technol.* **2013,** *47*, (17), 9781-9790.
(34) Writer, J. H.; Barber, L. B.; Ryan, J. N.; Bradley, P. M., Biodegradation and Attenuation of Steroidal Hormones and Alkylphenols by Stream Biofilms and Sediments. *Environ. Sci. Technol.* **2011,** *45*, (10), 4370-4376.

(35) Fono, L. J.; Kolodziej, E. P.; Sedlak, D. L., Attenuation of Wastewater-Derived Contaminants in an Effluent-Dominated River†. *Environ. Sci. Technol.* **2006,** *40*, (23), 7257-7262.
(36) Kunkel, U.; Radke, M., Fate of pharmaceuticals in rivers: Deriving a benchmark dataset at favorable attenuation conditions. *Water Research* **2012,** *46*, (17), 5551-5565.
(37) Aymerich, I.; Acuna, V.; Barcelo, D.; Garcia, M. J. J.; Petrovic, M.; Poch, M.; Rodriguez-Mozaz, S.; Rodriguez-Roda, I.; Sabater, S.; von Schiller, D.; Corominas, L., Attenuation of pharmaceuticals and their transformation products in a wastewater treatment plant and its receiving river ecosystem. *Water Research* **2016,** *100*, 126-136.
(38) Li, Z.; Sobek, A.; Radke, M., Fate of Pharmaceuticals and Their Transformation Products in Four Small European Rivers Receiving Treated Wastewater. *Environ. Sci. Technol.* **2016,** *50*, (11), 5614-5621.
(39) Acuña, V.; von Schiller, D.; García-Galán, M. J.; Rodríguez-Mozaz, S.; Corominas, L.; Petrovic, M.; Poch, M.; Barceló, D.; Sabater, S., Occurrence and in-stream attenuation of wastewater-derived pharmaceuticals in Iberian rivers. *Sci. Total Environ.* **2015,** *503–504*, 133-141.
(40) Hanamoto, S.; Nakada, N.; Yamashita, N.; Tanaka, H., Modeling the photochemical attenuation of down-the-drain chemicals during river transport by stochastic methods and field measurements of pharmaceuticals and personal care products. *Environ Sci Technol* **2013,** *47*, (23), 13571-7.
(41) Lewandowski, J.; Putschew, A.; Schwesig, D.; Neumann, C.; Radke, M., Fate of organic micropollutants in the hyporheic zone of a eutrophic lowland stream: results of a preliminary field study. *Sci Total Environ* **2011,** *409*, (10), 1824-35.
(42) Köhler, J.; Hachoł, J.; Hilt, S., Regulation of submersed macrophyte biomass in a temperate lowland river: Interactions between shading by bank vegetation, epiphyton and water turbidity. *Aquatic Botany* **2010,** *92*, (2), 129-136.
(43) Verleger; Schumacher, Auswirkungen von Maßnahmen zur Gewässerentwicklung und zur Verbesserung des Hochwasserschutzes in der Erpe auf den Grundwasserstand. *Erläuterungsbericht Staatsverwaltung für Stadtentwicklung und Umwelt, Berlin* **2012**.
(44) Schaper, J. L.; Seher, W.; Nutzmann, G.; Putschew, A.; Jekel, M.; Lewandowski, J., The fate of polar trace organic compounds in the hyporheic zone. *Water Res* **2018,** *140*, 158-166.
(45) Moschet, C.; Vermeirssen, E. L. M.; Singer, H.; Stamm, C.; Hollender, J., Evaluation of in-situ calibration of Chemcatcher passive samplers for 322 micropollutants in agricultural and urban affected rivers. *Water Research* **2015,** *71*, 306-317.
(46) Posselt, M.; Jaeger, A.; Schaper, J. L.; Radke, M.; Benskin, J. P., Determination of polar organic micropollutants in surface and pore water by high-resolution sampling-direct injection-ultra high performance liquid chromatography-tandem mass spectrometry. *Environmental Science: Processes & Impacts* **2018,** *20*, 1716-1727.
(47) Schwientek, M.; Guillet, G.; Rügner, H.; Kuch, B.; Grathwohl, P., A high-precision sampling scheme to assess persistence and transport characteristics of micropollutants in rivers. *Sci. Total Environ.* **2016,** *540*, 444-454.
(48) Leibundgut, C.; Maloszewski, P.; KÃ1⁄4lls, C., *Tracers in Hydrology*. Wiley: 2011.
(49) A., C. O.; N., F. M.; Markus, H.; Eduard, H.; Aronne, T.; Rolf, K.; K., K. P., Analyzing Bank Filtration by Deconvoluting Time Series of Electric Conductivity. *Groundwater* **2007,** *45*, (3), 318-328.
(50) Vogt, T.; Hoehn, E.; Schneider, P.; Freund, A.; Schirmer, M.; Cirpka, O. A., Fluctuations of electrical conductivity as a natural tracer for bank filtration in a losing stream. *Adv. Water Resour.* **2010,** *33*, (11), 1296-1308.
(51) Schreiber, I. M.; Mitch, W. A., Occurrence and fate of nitrosamines and nitrosamine precursors in wastewater-impacted surface waters using boron as a conservative tracer. *Environ Sci Technol* **2006,** *40*, (10), 3203-10.
(52) Conover, W.; Iman, R. L., On multiple-comparisons procedures. *Los Alamos Sci. Lab. Tech. Rep. LA-7677-MS* **1979**, 1-14.

(53) Benjamini, Y.; Krieger, A. M.; Yekutieli, D., Adaptive linear step-up procedures that control the false discovery rate. *Biometrika* **2006,** *93*, (3), 491-507.
(54) ter Laak, T. L.; Kooij, P. J. F.; Tolkamp, H.; Hofman, J., Different compositions of pharmaceuticals in Dutch and Belgian rivers explained by consumption patterns and treatment efficiency. *Environmental Science and Pollution Research* **2014,** *21*, (22), 12843-12855.
(55) Reemtsma, T.; Miehe, U.; Duennbier, U.; Jekel, M., Polar pollutants in municipal wastewater and the water cycle: occurrence and removal of benzotriazoles. *Water Res* **2010,** *44*.
(56) Kahl, S.; Kleinsteuber, S.; Nivala, J.; van Afferden, M.; Reemtsma, T., Emerging Biodegradation of the Previously Persistent Artificial Sweetener Acesulfame in Biological Wastewater Treatment. *Environ. Sci. Technol.* **2018,** *52*, (5), 2717-2725.
(57) Burke, V.; Greskowiak, J.; Asmuß, T.; Bremermann, R.; Taute, T.; Massmann, G., Temperature dependent redox zonation and attenuation of wastewater-derived organic micropollutants in the hyporheic zone. *Sci. Total Environ.* **2014,** *482–483*, 53-61.
(58) Schwarzenbach, R. P.; Gschwend, P. M.; Imboden, D. M., Biological Transformations. In *Environmental Organic Chemistry*, John Wiley & Sons, Inc.: 2005; pp 687-773.
(59) Jude, K. A.; Giorgio, P. A. d.; Kemp, W. M., Temperature regulation of bacterial production, respiration, and growth efficiency in a temperate salt-marsh estuary. *Aquatic Microbial Ecology* **2006,** *43*, (3), 243-254.
(60) Comer-Warner, S. A.; Romeijn, P.; Gooddy, D. C.; Ullah, S.; Kettridge, N.; Marchant, B.; Hannah, D. M.; Krause, S., Thermal sensitivity of CO2 and CH4 emissions varies with streambed sediment properties. *Nature Communications* **2018,** *9*, (1), 2803.
(61) Bonvin, F.; Omlin, J.; Rutler, R.; Schweizer, W. B.; Alaimo, P. J.; Strathmann, T. J.; McNeill, K.; Kohn, T., Direct photolysis of human metabolites of the antibiotic sulfamethoxazole: evidence for abiotic back-transformation. *Environ Sci Technol* **2013,** *47*, (13), 6746-55.
(62) Radke, M.; Lauwigi, C.; Heinkele, G.; Murdter, T. E.; Letzel, M., Fate of the antibiotic sulfamethoxazole and its two major human metabolites in a water sediment test. *Environ Sci Technol* **2009,** *43*, (9), 3135-41.
(63) Li, Z.; Maier, M. P.; Radke, M., Screening for pharmaceutical transformation products formed in river sediment by combining ultrahigh performance liquid chromatography/high resolution mass spectrometry with a rapid data-processing method. *Analytica Chimica Acta* **2014,** *810*, 61-70.
(64) Zhang, T.; Pan, G.; Zhou, Q., Temperature effect on photolysis decomposing of perfluorooctanoic acid. *Journal of environmental sciences (China)* **2016,** *42*, 126-133.
(65) Kern, S.; Baumgartner, R.; Helbling, D. E.; Hollender, J.; Singer, H.; Loos, M. J.; Schwarzenbach, R. P.; Fenner, K., A tiered procedure for assessing the formation of biotransformation products of pharmaceuticals and biocides during activated sludge treatment. *Journal of Environmental Monitoring* **2010,** *12*, (11), 2100-2111.
(66) Bartell, F. E.; Thomas, T. L.; Fu, Y., Thermodynamics of Adsorption from Solutions. IV. Temperature Dependence of Adsorption. *The Journal of Physical Chemistry* **1951,** *55*, (9), 1456-1462.
(67) Alidina, M.; Shewchuk, J.; Drewes, J. E., Effect of temperature on removal of trace organic chemicals in managed aquifer recharge systems. *Chemosphere* **2015,** *122*, 23-31.
(68) Helbling, D. E.; Hollender, J.; Kohler, H. P.; Singer, H.; Fenner, K., High-throughput identification of microbial transformation products of organic micropollutants. *Environ Sci Technol* **2010,** *44*, (17), 6621-7.
(69) Rubirola, A.; Llorca, M.; Rodriguez-Mozaz, S.; Casas, N.; Rodriguez-Roda, I.; Barceló, D.; Buttiglieri, G., Characterization of metoprolol biodegradation and its transformation products generated in activated sludge batch experiments and in full scale WWTPs. *Water Research* **2014,** *63*, 21-32.
(70) Gonzalez-Pinzon, R.; Peipoch, M.; Haggerty, R.; Marti, E.; Fleckenstein, J. H., Nighttime and daytime respiration in a headwater stream. *Ecohydrology* **2016,** *9*, (1), 93-100.

(71) Nodler, K.; Tsakiri, M.; Licha, T., The impact of different proportions of a treated effluent on the biotransformation of selected micro-contaminants in river water microcosms. *Int J Environ Res Public Health* **2014,** *11*, (10), 10390-405.
(72) Trautwein, C.; Kümmerer, K., Incomplete aerobic degradation of the antidiabetic drug Metformin and identification of the bacterial dead-end transformation product Guanylurea. *Chemosphere* **2011,** *85*, (5), 765-773.
(73) Gartiser, S.; Hafner, C.; Kronenberger-Schafer, K.; Happel, O.; Trautwein, C.; Kummerer, K., Approach for detecting mutagenicity of biodegraded and ozonated pharmaceuticals, metabolites and transformation products from a drinking water perspective. *Environmental science and pollution research international* **2012,** *19*, (8), 3597-609.
(74) Briones, R. M.; Sarmah, A. K., Detailed sorption characteristics of the anti-diabetic drug metformin and its transformation product guanylurea in agricultural soils. *Sci Total Environ* **2018,** *630*, 1258-1268.

Supporting Information for

Spatial and temporal variability in attenuation of polar organic micropollutants in an urban lowland stream

Jaeger Anna*‡ (1,2), Posselt Malte‡ (3), Betterle Andrea (4,5,6), Schaper Jonas (1,7), Mechelke Jonas (4,8), Coll Claudia (3), Lewandowski Joerg (1,2)

‡These authors contributed equally to the work

(1) Leibniz-Institute of Freshwater Ecology and Inland Fisheries, Department Ecohydrology, Berlin, Germany
(2) Humboldt University Berlin, Geography Department, Berlin, Germany
(3) Stockholm University, Department of Environmental Science and Analytical Chemistry, Stockholm, Sweden
(4) Eawag, Swiss Federal Institute of Aquatic Science and Technology, Department of Water Resources and Drinking Water, Dübendorf, Switzerland
(5) University of Neuchâtel, Centre of Hydrogeology and Geothermics, Neuchâtel, Switzerland
(6) University of Padova, Department of ICEA and International Center for Hydrology, Padua, Italy
(7) Technical University of Berlin, Chair of Water Quality Engineering, Berlin, Germany
(8) ETH Zürich, Institute of Biogeochemistry and Pollutant Dynamics, Zürich, Switzerland

***Corresponding author:**

Anna Jaeger

Leibniz-Institute of Freshwater Ecology and Inland Fisheries, Department Ecohydrology, Berlin, Germany and Humboldt University Berlin, Geography Department, Berlin, Germany

E-mail: anna.jaeger@igb-berlin.de

Contents:

Pages: 21

Tables: 9

Figures: 8

Background information and data

The WWTP facility has a dry weather capacity of 220,000 population equivalents and includes denitrification and chemical phosphorous precipitation.[1] Sampling station A was located at 52°28'48.3"N 13°38'12.4"E, station B at 52°28'13.2"N 13°37'24.7"E and station C at 52°45'51.0"N, 13°59'75.1"E. Complete mixing of the river water and the WWTP effluent at station A is assured according to a method calculating the mixing length reported in a USGS guidline.[2] Discharge at the sampling sites was determined by discharge-water stage rating curves, using an Acoustic Doppler Current Profiler (StreamPro ADCP by Teledyne RD Instruments, La Gaude, France) for discharge measurements. Average discharge during sampling periods decreased from station A (0.69 $m^3 s^{-1}$) to station B (0.61 $m^3 s^{-1}$) to station C (0.47 $m^3 s^{-1}$). The cause of the loss in S2 remains unclear. Average discharge was 13% lower *am* (0.55 $m^3 s^{-1}$) than *bm* (0.63 $m^3 s^{-1}$). Biased discharge estimates at station C might result from measurement uncertainties, as the wide channel and low flow velocities at this location hindered the establishment of a robust rating curve.

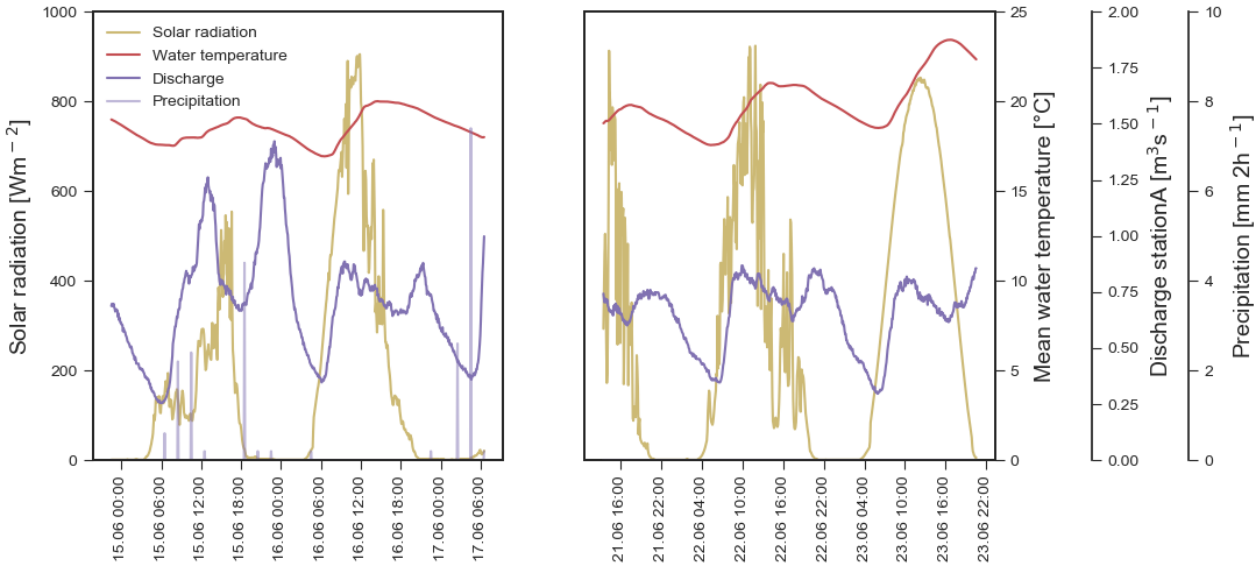

Figure S1 Background weather and flow-data recorded during the sampling periods before and after mowing (bm and am). Solar radiation and precipitation were recorded at a weather station located 2.6 km south-east of the river. Water temperature was recorded at all stations and averaged. The discharge time series was calculated based on the water level at station A and a measured water level-discharge relationship.

Dissolved organic carbon (DOC) was only measured in selected samples. Subsamples for analysis of dissolved organic carbon (DOC) were filtered (0.45 µm cellulose acetate), stored at 4 °C and measured by NDIR after combustion DIN EN 1484 (DEV, H3) at a TOC Analyzer (Shimadzu). In average it increased slightly in S1 (11.4 to 11.7 mg L^{-1}) and remained constant in S2 (11.7 mg L^{-1}). Average DOC was slightly higher *am* (12.0 mg L^{-1}) than *bm* (11.1 mg L^{-1}). Nitrate and sulfate was measured in every other sample. Subsamples for analysis of nitrate were filtered immediately after sampling (0.2 µm cellulose acetate), stored at -20 °C and measured by ionchromatography after DIN EN ISO 10304-1 (Shimadzu). Subsamples for analysis of phosphorous, calcium, magnesium, potassium and sodium were filtered immediately after sampling (0.45 µm cellulose acetate), acidified with HCl, stored at 4 °C and measured by inductively coupled plasma optical emission spectrometry (ICP iCAP

6000series, Thermo Fisher Scientific Inc.). A summary of average concentrations of background data within the sampling situations is presented in

Table S1. The pH was determined in selected samples using a handheld pH meter, calibrated prior to each use (SenTix 41, WTW). It was measured to be in average 7.9±0.1 *bm* and 7.7±0.1 *am*.

Table S1 Average values ± standard deviation of background parameters measured in the four sampling situations.

		S1bm	**S1am**	**S2bm**	**S2am**
Solar radiation	[W m^{-2}]	189 ±234	278 ±301	189 ±350	284 ±345
Water temperature	[° C]	18.5 ±0.9	19.5 ±1.4	18.6 ±0.9	19.9 ±1.8
Discharge	[m^3 s^{-1}]	0.71 ±0.2	0.59 ±0.1	0.58 ±0.2	0.50 ±0.1
DOC	[mg L^{-1}]	11.0 ±0.9	12.1 ±1.8	11.3 ±0.8	12.1 ±1.5
Nitrate-N	[mg L^{-1}]	7.3 ±0.9	6.8 ±0.6	7.2 ±0.8	6.9 ±0.6
Sulfate	[mg L^{-1}]	126 ±8.5	134 ±5.8	127 ±7.4	137 ±4.7
Total Phosphorous	[mg L^{-1}]	0.46 ±0.06	0.40 ±0.04	0.46 ±0.05	0.38 ±0.03
Calcium	[mg L^{-1}]	94.2 ±6.8	99.3 ±7.5	96.0 ±6.2	99.5 ±7.4
Magnesium	[mg L^{-1}]	11.0 ±0.9	11.4 ±0.7	11.3 ±0.8	11.4 ±0.7
Potassium	[mg L^{-1}]	24.4 ±3.4	25.1 ±1.7	24.9 ±3.2	25.0 ±1.5
Sodium	[mg L^{-1}]	92.1 ±11.8	88.6 ±7.9	93.6 ±11.1	88.4 ±7.6

Figure S2 Photograph of macrophyte removal at River Erpe roughly 1 km downstream of the WWTP inflow (Friday, 17.06.2016). Water level was extraordinary high after short, heavy rainfall.

Quality control and quality assurance of TrOC analysis

Three different blank samples were measured to control for contamination and false positives: surface water from upstream of the WWTP inflow was collected once every four hours during sampling as a field blank. In addition, tap water and Milli-Q-water was processed like normal samples. No TrOCs were detected in Milli-Q and tap water. Low concentrations of acesulfame, carbamazepine, 10,11-dihydro-10,11-dihydroxy carbamazepine and valsartan acid were detected in upstream surface water (data presented in Posselt et al.[3]). Samples were measured directly after method validation and the same matrix was used. Therefore, accuracy and precision values as presented in Posselt et al.[3] apply. Instrumental repeatability and reproducibility was excellent; Mean recovery data are presented in Figure S3 and precision data in Table S9.

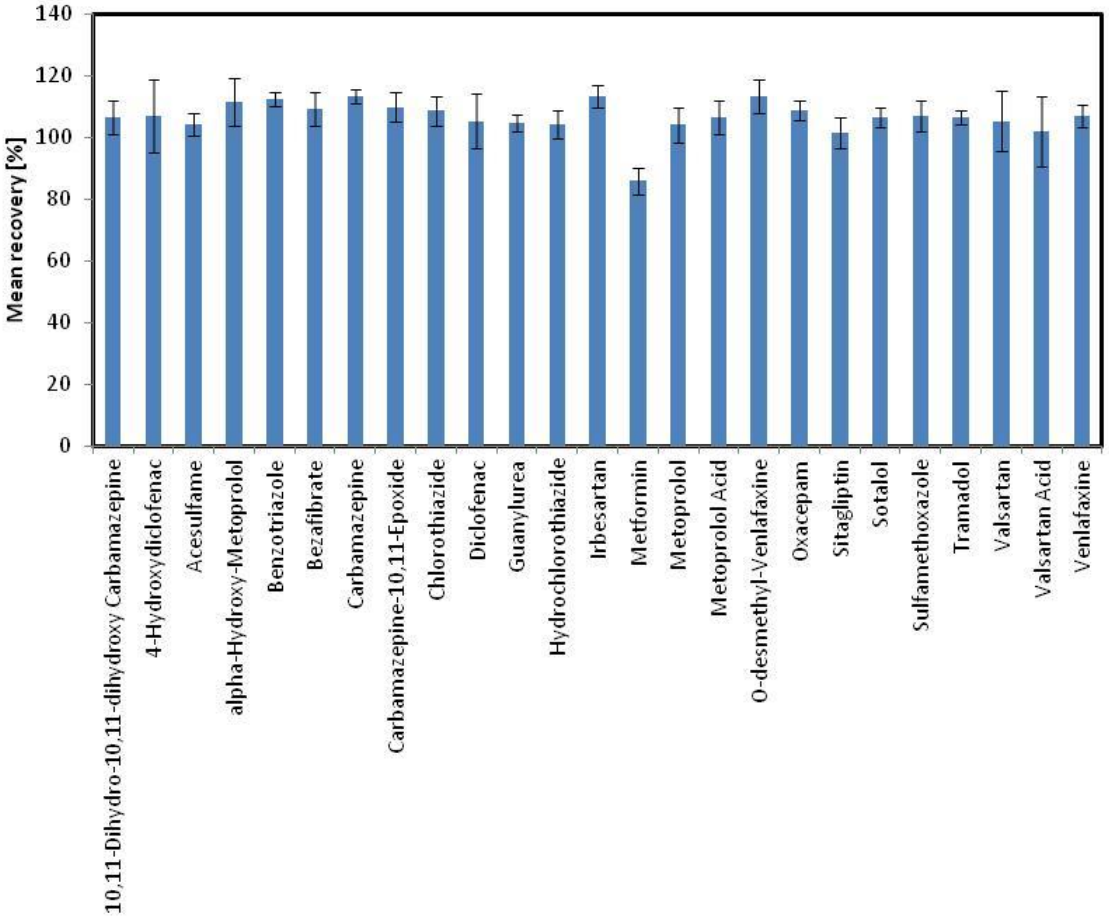

Figure S3 All water samples of this study were measured within the course of one week. Data for within-batch repeatability over this period of time: mean recovery ± % RSD of a quality control standard (Milli-Q water) that was measured every 15-20 samples (N=19). The standard concentrations were compound specific and between 1 and 2.5 µg L^{-1} i.e. mostly at the lower end of measured Erpe concentration ranges.

Details on deconvolution of electrical conductivity

The method statistically computes the transfer function (i.e. the residence time distribution) that once applied to the measured EC signal at an upstream location can best reproduce the observed time variability of the EC signal at a downstream site. The method assumes the stream as a linear time-invariant operator which smooths and shifts the input EC signal (assumed as a conservative tracer) and helps revealing the transport characteristics of the stream. The peak time of the transfer function is mainly controlled by advective processes whereas dispersion or transient storage processes can affect the spreading of the residence time distribution.[4,5] Dispersion of the residence time distribution might also be related to unsteady flow conditions resulting from the input of treated wastewater. The method doesn't assume any parametric structure of the residence time and is therefore more flexible and suited to capture a broad spectrum of residence time distributions. Additionally, by using entire time series of EC, the method can account for the travel time variability caused by unsteady transport processes during the recorded period. A reduction of the time to peak as well as a reduced spreading of the residence time distribution is observed in the absence of macrophytes in S1. The increase in time to peak in S2am compared to S2bm is attributed to lower average discharge in the sampling days after mowing.

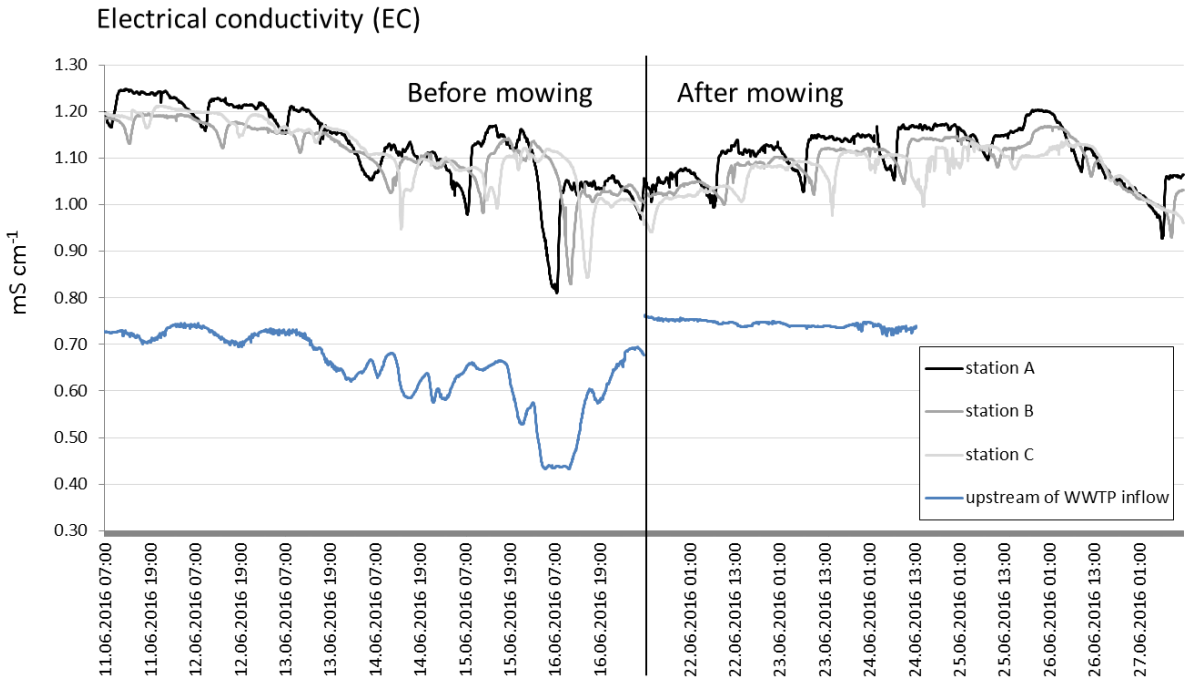

Figure S4 Electrical conductivity fluctuations time series at station A, B and C (greys) before and after mowing (17.06.2016 10:00). For comparison, EC in the river water 80 m upstream of the WWTP inflow is shown in blue (Aqua TROLL 200, In-Situ Inc., Fort Collins, USA), data after 24.06.2016 13:00 are missing due to technical problems.

Determination of parcel-specific water temperature and solar radiation

To calculate each parcel's theoretical exposure to solar radiation (SR_p) disregarding any shading, the global solar radiation (sr_i) recorded at the weather station of Leibniz Institute of Freshwater Ecology and Inland Fisheries, Berlin (52°26'55.7"N 13°38'50.2"E) in 5 minutes intervals (m) during the individual travel period of the parcels (t_{start} to $t_{start}+t_p$) was averaged.

$$SR_p = \frac{1}{t_p * m^{-1}} \sum_{i=t_{start}}^{t_p * m^{-1}} sr_i$$

The average temperature a single water parcel was exposed to (WT_p) was calculated by averaging the average of water temperature ($wt_{i,in}$) measured by data loggers in 5 minute intervals (m) at the upstream station during the first half (startin g at t_{start}) of the travel period (t_p) and the average of water temperature ($wt_{i,out}$) at the downstream station during the second half of the travel period (starting at t_{mid}).

$$WT_p = \frac{1}{2}\left[\left(\frac{1}{t_p * 2^{-1} * m^{-1}} \sum_{i=t_{start}}^{t_p * 2^{-1} * m^{-1}} wt_{i,in}\right) + \left(\frac{1}{t_p * 2^{-1} * m^{-1}} \sum_{i=t_{mid}}^{t_p * 2^{-1} * m^{-1}} wt_{i,out}\right)\right]$$

Table S2 Results from Kruskal-Wallis tests and Conover tests as post-hoc tests to test differences in k_{att} between sampling situations, as well as Shapiro-Wilk test to test normality of single distributions.

Compound (parent compounds are highlighted in bold, related TPs are listed below)	Kruskal-Wallis test		Post-hoc test by Conover with two-stage p-value correction by Benjamini, Krieger and Yekuteli				Shapiro-Wilk test for normality			
	P-value	H statistic, corrected for ties	P-value S1bm vs. S1am	P-value S1bm vs. S2bm	P-value S2bm vs. S2am	P-value S1am vs. S2am	P-value S1bm	P-value S1am	P-value S2bm	P-value S2am
Acesulfame	0.175	5.0					0.019	0.387	0.263	0.144
1H-Benzotriazole	0.027	9.2	0.081	0.819	0.089	0.828	0.022	0.340	0.020	0.492
Bezafibrate	6.34E-03	12.3	0.099	0.139	0.457	0.010	0.024	0.062	0.307	3.54E-03
Carbamazepine	0.466	2.5					0.086	0.177	0.284	0.129
10,11-Dihydro-10,11-dihydroxy Carbamazepine	0.605	1.8					0.177	0.091	0.189	0.346
Carbamazepine-10,11-Epoxide	0.261	4.0					0.431	0.084	0.029	0.378
Diclofenac	3.70E-03	13.5	0.032	0.168	0.077	0.077	0.020	0.158	0.016	0.016
4-Hydroxydiclofenac	1.92E-07	34.1	4.85E-04	4.67E-04	2.37E-04	1.27E-03	1.12E-03	6.42E-04	5.29E-05	6.16E-04
Hydrochlorothiazide	2.05E-06	29.2	2.22E-07	0.073	0.051	4.28E-03	3.64E-07	0.143	0.063	2.32E-03
Chlorothiazide	0.110	6.0					0.106	6.39E-03	0.052	0.378
Irbesartan	0.054	7.7					0.021	0.393	0.027	0.360
Metformin	0.139	5.5					0.022	0.270	0.253	0.070
Guanylurea	1.05E-06	30.6	1.40E-06	0.233	0.239	1.89E-06	1.55E-06	0.173	0.187	1.26E-06
Metoprolol	1.29E-07	34.9	0.018	9.92E-8	0.178	1.84E-03	0.020	7.74E-07	0.177	2.21E-03
α-Hydroxymetoprolol	0.174	5.0					0.125	0.248	0.369	0.024
Metoprolol Acid	1.02E-04	21.1	0.048	2.22E-05	0.094	0.094	0.122	5.34E-06	0.049	0.151
Sitagliptin	0.187	4.8					0.072	0.324	0.127	5.31E-03
Sotalol	0.224	4.4					0.048	0.203	0.294	0.127
Sulfamethoxazole	1.20E-05	25.5	0.096	2.66E-06	8.05E-03	8.05E-03	0.295	3.78E-06	0.007	0.010
Tramadol	0.200	4.6					0.027	0.310	0.387	0.102
Valsartan	8.16E-04	16.7	0.204	5.17E-04	0.154	0.060	0.212	1.34E-04	0.113	0.042
Valsartan Acid	6.13E-04	17.3	0.613	0.104	0.052	8.11E-04	0.419	0.027	0.031	1.74E-04
Venlafaxine	0.862	0.7					0.277	0.262	0.428	0.431
O-Desmethylvenlafaxine	0.188	4.8					0.175	0.155	0.145	0.086

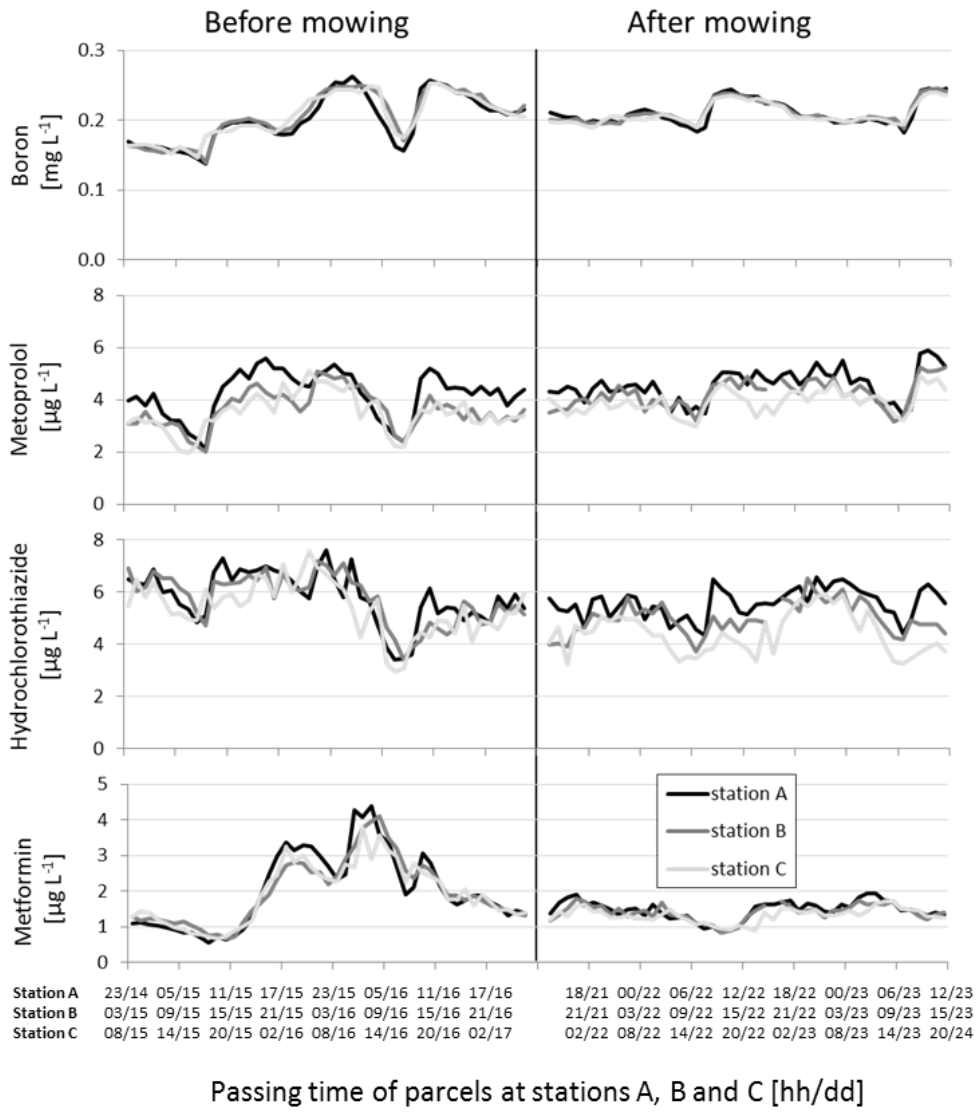

Figure S5 Concentrations of boron, metoprolol, hydrochlorothiazide and metformin in the sequence of single water parcels at station A, B and C, respectively. The x-axis depicts the times the water parcel is passing the single stations.

Passive sampling

From the 5th to the 16th of June (bm) and the 20th to the 30th of June (am) 2016 Chemcatcher® passive samplers in polar configuration were deployed at stations A, B and C in duplicates. The used Chemcatcher® configuration, i.e. a Empore™ reversed-phase sulfonated styrenedivinylbenzene disk (SDB-RPS, 47 mm diameter, Sigma Aldrich) covered by diffusion limiting polyethersulfone -membrane (PES, 0.10 μm pore size, Sigma Aldrich), is suitable for the enrichment of polar and semi-polar organic compounds with log K_{OW} values between approximately -2 and 5.[6] For the field installation, SDB-RPS disks were placed on steel plates (70 by 100 mm), covered by PES membranes, closed by cover plates (70 by 70 mm), and stored in Nanopure® water at room temperature until deployment. After deployment in the field, SDB-RPS disks were recovered from river Erpe, carefully dried, stored at -20 °C until transport to Switzerland in a cooling box with dry ice. Upon arrival, SDB-RPS disks were put in 6 mL acetone and stored at -20 °C until extraction and analysis.

Analysis of TrOCs was conducted at EAWAG Zurich, Switzerland, by an established method for passive samplers. In this method, 17 of the 24 TrOCs measured in the water samples at Stockholm University, Sweden, were included (Table S4). For the extraction, SDB-RPS disks in acetone were allowed to equilibrate to room temperature and shaken on a rotary shaker for 60 min. The obtained extracts were transferred to new vials and an internal standard mix was added. SDB-RPS disks were extracted a second time for 60 min with 6 mL methanol. The first SDB-RPS disk extract (acetone) was reduced to roughly 1 mL using nitrogen blowdown (40°C) and combined with the second extract (methanol). The extracts were filtered (PTFE, 0.45 μm pore size). The filtered extract of one duplicate per site was split by weight and fortified with analyte standards in order to calculate the relative recovery, i.e. the analyte spike recovery. Unspiked and spiked extracts were evaporated to 0.1 and 0.05 mL, respectively, and reconstituted to 1 and 0.5 mL, respectively, using Nanopure® water. Extracts were measured by liquid chromatography high-resolution tandem mass spectrometry (LC-HRMS/MS) using an Atlantis T3 (Waters, Milford MA, USA) reversed-phase C18 column (3 x 150 mm, 3 μm) for chromatographic separation, an electrospray ionization (ESI) interface, and a QExactive Plus (Thermo Scientific, USA) mass spectrometer (MS). The injection volume was set to 100 μL. Water and methanol both acidified with 0.1% formic acid, were used as eluents for the chromatographic gradient. Mass spectra were acquired in full-scan mode at a mass resolution (R) of 140'000 (FWHM, m/z 400) with subsequent data-dependent MS2 (Top5, R = 17'500), carrying out separate runs for positive and negative ESI. Analytes of interest were quantified with TraceFinder 4.1 (Thermo Scientific, USA) using internal calibration. Since most target analytes were prone to positive ESI, only raw files measured in positive ESI mode were evaluated.

Experimental polar Chemcatcher® sampling rates (data not shown) and field sampling rates taken from literature[7] were used to calculate time-weighted average concentrations of analytes in the Erpe water based on the amounts of analytes accumulated in the receiving phase (SDB-RPS disk) during the exposure periods. In previous studies[7], no pronounced effect of flow on uptake has been reported for the majority of analytes above a flow velocity of approx. 0.1 m s^{-1}. Mean flow velocities during the exposure periods ranged from 0.05 to 0.3 m s^{-1} (see Table S3) and were greater 0.1 m s^{-1} except at station C. This might slightly overestimate katt between stations B and C (S2). However, since the sampling rates are usually only valid under the respective flow conditions or field flow conditions, the calculated water concentrations are only an estimate.

A list of compounds analysed in both methods is provided in Table S4. To obtain a k_{att} estimated by the passive samplers comparable to those calculated in the 48 water parcels, the concentrations of the duplicates were averaged and used as in- and output concentration as applied for the water parcels (Eq. 1). The same travel times were used. A correction of concentrations with a conservative tracer was not applied. Precipitation during the deployment periods of the passive samplers was low (0.1 mm h^{-1} *bm* and 0.03 mm h^{-1} *am*), thus no considerable dilution was expected. Concentrations and resulting k_{att} estimated by the passive samplers in the four situations are listed in Table S4.

Table S3 Mean flow velocities during deployment periods of the passive samplers *am* and *bm* at the three sampling stations, measured by StreamPro ADCP by Teledyne RD Instruments, La Gaude, France.

	Mean flow velocity [m s^{-1}]	
	***bm* (5-16.6.2016)**	***am* (20-30.6.2016)**
Station A	0.242	0.317
Station B	0.163	0.158
Station C	0.054	0.079

Table S4 Average concentrations estimated from passive sampler duplicates and standard deviation, as well as resulting k_{att} and uncertainty calculated by uncertainty propagation of the concentration standard deviations in the four sampling situations. The analysis of the TrOCs collected by the passive samplers was conducted at EAWAG Zurich, Switzerland and the method included 17 out of the 24 compounds analysed in the water samples at Stockholm University, Sweden. * Dh-Carbamazepine = 10,11-Dihydro-10,11-dihydroxy Carbamazepine.

Compound	Conc. bm station A [µg L^{-1}]	Conc. bm station B [µg L^{-1}]	Conc. bm station C [µg L^{-1}]	Conc. am station A [µg L^{-1}]	Conc. am station B [µg L^{-1}]	Conc. am station C [µg L^{-1}]	k_{att} S1bm [h^{-1}]	k_{att} S1am [h^{-1}]	k_{att} S2bm [h^{-1}]	k_{att} S2am [h^{-1}]
1H-Benzotriazole	8.09 ±0.04	8.11 ±0.25	7.38 ±0.19	8.43 ±0.10	8.37 ±0.24	8.22 ±0.15	(-0.0006) ±0.007	0.0024 ±0.010	0.0210 ±0.009	0.0034 ±0.006
Bezafibrate	0.53 ±0.03	0.48 ±0.001	0.43 ±0.01	0.56 ±0.02	0.52 ±0.01	0.48 ±0.02	0.0219 ±0.012	0.0257 ±0.011	0.0218 ±0.005	0.0142 ±0.009
Carbamazepine	1.37 ±0.10	1.51 ±0.04	1.37 ±0.12	1.37 ±0.04	1.38 ±0.19	1.21 ±0.02	(-0.0226) ±0.017	(-0.0026) ±0.045	0.0215 ±0.02	0.0248 ±0.026
Dh-Carbamazepine*	0.00 ±0.0	0.00 ±0.0	0.00 ±0.0	0.97 ±0.08	0.90 ±0.03	0.80 ±0.02	na	0.0248	na	0.0208
Carbamazepine -10,11-Epoxide	0.29 ±0.01	0.27 ±0.04	0.23 ±0.01	0.26 ±0.01	0.25 ±0.000	0.25 ±0.003	0.0086 ±0.008	0.0095 ±0.007	0.0356 ±0.014	0.0040 ±0.002
Diclofenac	3.21 ±0.02	3.07 ±0.11	2.76 ±0.11	3.13 ±0.26	2.74 ±0.05	2.48 ±0.15	0.0104 ±0.009	0.0429 ±0.028	0.0236 ±0.012	0.0183 ±0.012
4-Hydroxydiclofenac	0.87 ±0.10	0.65 ±0.08	0.45 ±0.01	0.75 ±0.01	0.50 ±0.04	0.39 ±0.02	0.0669 ±0.039	0.1324 ±0.023	0.0791 ±0.028	0.0461 ±0.017
Irbesartan	1.57 ±0.01	1.64 ±0.06	1.44 ±0.10	1.49 ±0.09	1.43 ±0.002	1.33 ±0.04	(-0.0100) ±0.008	0.0145 ±0.019	0.0279 ±0.017	0.0130 ±0.006
Metformin	4.17 ±0.18	3.84 ±0.16	3.37 ±0.15	6.11 ±0.55	6.09 ±0.33	5.49 ±0.24	0.0184 ±0.013	0.0011 ±0.034	0.0294 ±0.013	0.0194 ±0.013
Guanylurea	24.3 ±3.1	21.3 ±1.4	20.0 ±1.7	20.2 ±0.7	19.5 ±1.8	18.6 ±4.3	0.0300 ±0.033	0.0117 ±0.032	0.0141 ±0.024	0.0095 ±0.046
Metoprolol	6.24 ±0.18	4.84 ±0.20	4.50 ±0.43	6.72 ±0.86	6.14 ± 0.10	4.99 ±0.34	0.0578 ±0.011	0.0295 ±0.042	0.0161 ±0.023	0.0384 ±0.013
Metoprolol Acid	0.29 ±0.01	0.39 ±0.01	0.40 ±0.02	0.41 ±0.04	0.40 ±0.01	0.41 ±0.07	(-0.0679) ±0.006	0.0100 ±0.035	(-0.0045) ±0.009	(-0.0042) ±0.032
Sitagliptin	5.07 ±0.09	4.95 ±0.24	4.71 ±0.29	5.01 ±0.33	4.73 ±0.02	4.57 ±0.001	0.0052 ±0.012	0.0186 ±0.021	0.0110 ±0.018	0.0065 ±0.001
Sulfamethoxazole	0.47 ±0.004	0.48 ±0.004	0.48 ±0.002	0.45 ±0.01	0.45 ±0.004	0.49 ±0.02	(-0.0050) ±0.003	(-0.0001) ±0.008	(-0.0017) ±0.002	(-0.0156) ±0.008
Tramadol	2.80 ±0.07	2.53 ±0.004	2.87 ±0.34	2.93 ±0.38	2.90 ±0.05	2.72 ±0.11	0.0226 ±0.006	0.0027 ±0.042	(-0.0282) ±0.026	0.0118 ±0.008
Valsartan	13.32 ±0.05	10.31 ±0.28	8.98 ±1.10	14.48 ±0.69	12.58 ±1.34	11.40 ±0.16	0.0579 ±0.006	0.0457 ±0.038	0.0306 ±0.028	0.0181 ±0.02
Venlafaxine	0.42 ±0.02	0.40 ±0.003	0.47 ±0.08	0.47 ±0.08	0.48 ±0.02	0.42 ±0.01	0.0140 ±0.012	(-0.0020) ±0.059	(-0.0357) ±0.036	0.0238 ±0.007

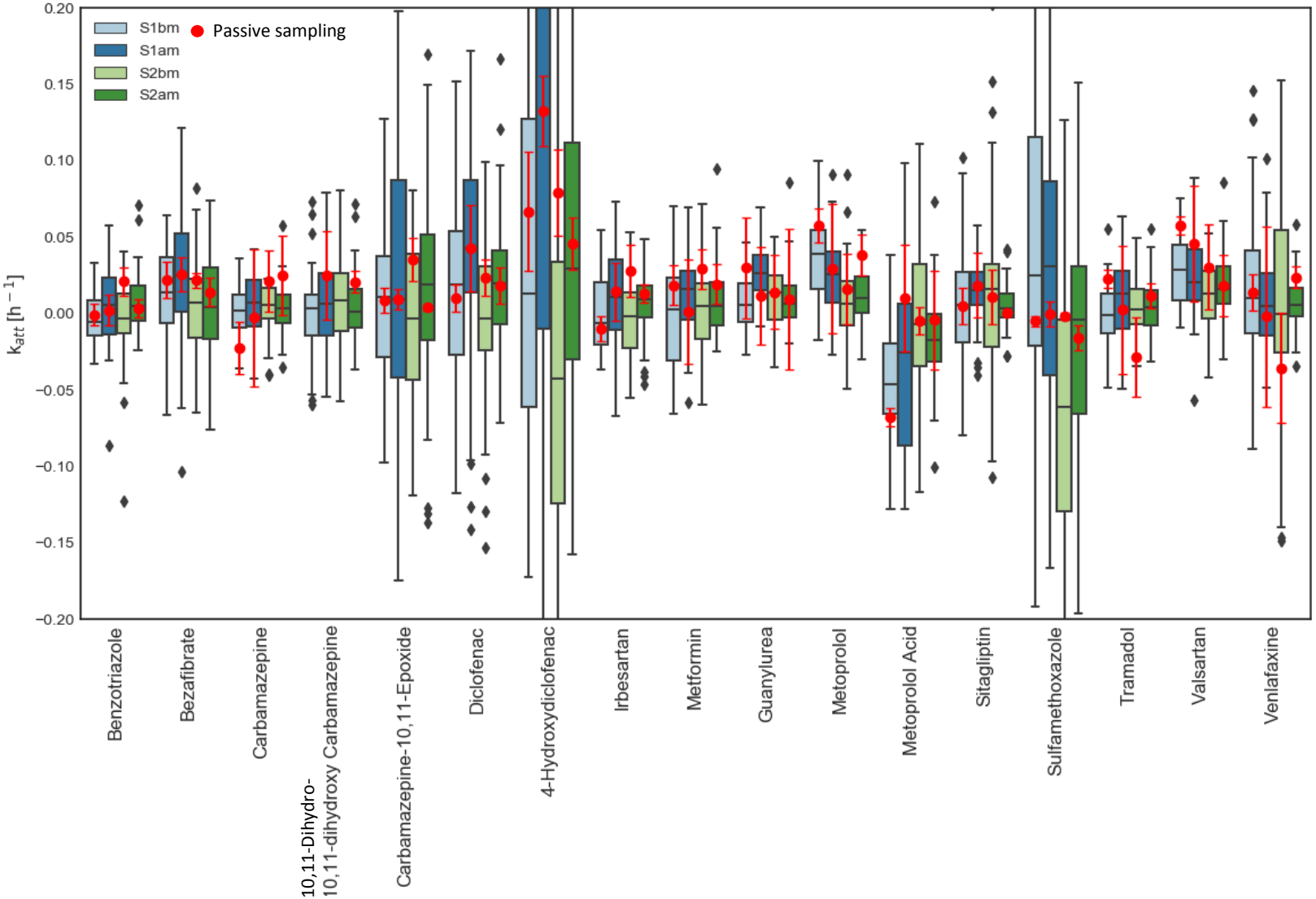

Figure S6 Comparison of 10/11-day average k_{att} measured by the passive samplers (red dots, error bars indicate uncertainty calculated from uncertainty propagation of the concentration standard deviations) and the 48-hour distributions of k_{att} measured in the water samples.

A direct comparison between the results for TrOC attenuation from the passive sampler (11/10-day k_{att}) and the high-resolution sampling (2-day k_{att}) has to be interpreted with caution, as for the different uncertainties associated with the analytical methods and the calculation of k_{att}. However, some general findings are noteworthy: The 11/10-day k_{att} of all compounds lies within the distribution of the 2-day k_{att} in all sampling situations. Most of the times, it even lies within the inter quartile range (boxes in Figure S6). The k_{att} averaged over all sampling situations of the single compounds correlates well between the two methods (Figure S7). This means general reactivity of the compounds coincides well between the two methods. Looking at the distinct situations, in S1bm, S1am and S2am, the 2-day median k_{att} and the 11/10-day k_{att} are generally positively correlated (Figure S8). Only in S2bm they are not in line. An explanation could be the difference in average solar radiation between the 2-day and the 11-day sampling periods *bm* (Table S5). The weather differences might be less relevant for S1 than S2 due to the prevailing effect of the macrophytes. Most (13 out of 17) compounds analysed in both methods show the same trend between S1bm and S1am in the 11/10-week average k_{att} and the 2-day median k_{att} (Figure S6). This indicates that the differences in attenuation in S1 observed between the 2-day sampling periods *bm* and *am* are caused by a longer-lasting phenomenon. Thus, the processes attributed to macrophyte removal are not merely short-term effects and overlay the meteorological differences between the sampling periods. Exceptions are metformin, guanylurea and tramadol. Those compounds show similar trends in their median 2-day k_{att} and all are charged positively under ambient pH (Table S8). This suggests that the three of them are susceptible to similar processes and the change in trend between the 2- and 11/10-day k_{att} might be caused by a short-term change in sorption conditions. Differences in S1am and S2am in 2-day k_{att}, attributed to higher photolysis and transient storage potential in S1 is reflected in the 10-day k_{att} for 10 of the compounds, including the photosensitives diclofenac and 4-hydroxydiclofenac. The trend is reversed again for metformin, guanylurea and tramadol. But also for carbamazepine, carbamazepine-10,11-epoxide, metoprolol, metoprolol acid and venlafaxine. An explanation remains speculative, but again sorption could play a role, as metformin, guanylurea, tramadol, metoprolol and venlafaxine are positively charged (Table S8).

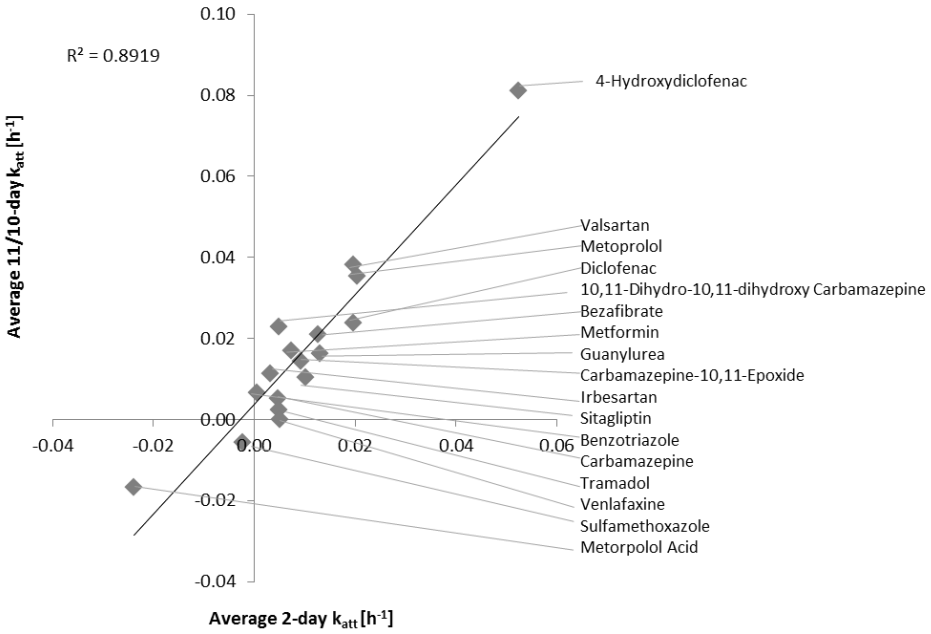

Figure S7 Relation between 11/10-day k_{att} and 2-day median k_{att} averaged over the sampling situations S1bm, S1am, S2bm and S2am.

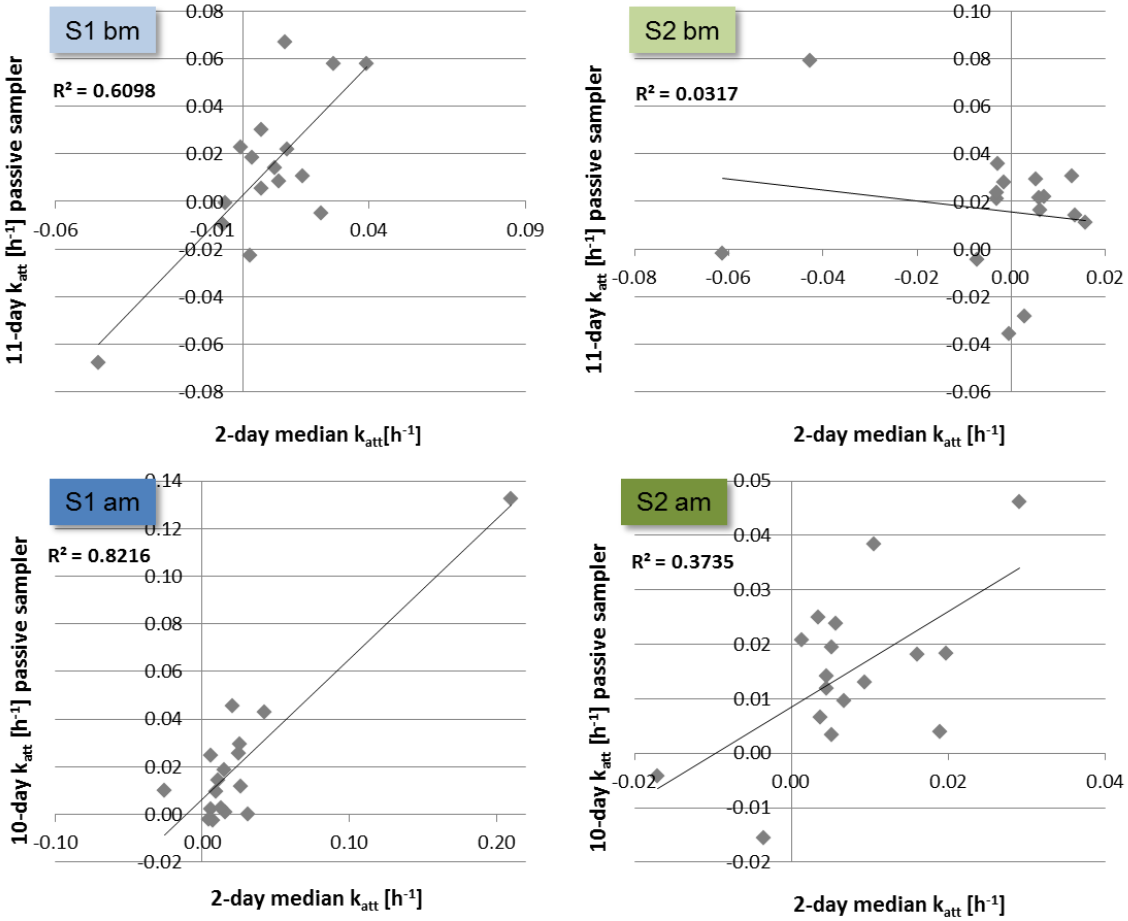

Figure S8 Relation between 2-day median and 11/10-day k_{att} in the four sampling situations of all compounds measured in both methods.

Table S5 comparing the average solar radiation and water temperature in the sampling periods of the passive samplers (11/10 days) with the data in the sampling periods of the autosamplers (48 hours).

		S1bm	S2bm	S1am	S2am	Differences *bm*	Differences *am*
Solar radiation	48-hour average	189 ±234	189 ±350	278 ±301	284 ±345	+26%	-8%
	10/11-day average	239 ±285		259 ±291			
Water temper-ature	48-hour average	18.5 ±0.9	18.6 ±0.9	19.5 ±1.4	19.9 ±1.8	+4%	+3%
	10/11-day average	19.2 ±1.4		20.2 ±1.8			

Table S6 Quartiles of distributions, median half-lifes and median relative attenuation of all compounds in S1bm, S1am, S2bm and S2am, respectively.

Compound (parent compounds are highlighted in bold, related TPs are listed below)	Distribution of k_{att} 1st/3rd quartile (Q) and interquartile range (IQR) [h^{-1}]												Median DT50 (half-lifes) [h]				Median relative attenuation			
	S1bm			S1am			S2 bm			S2am										
	1st Q	3rd Q	IQR	1st Q	3rd Q	IQR	1st Q	3rd Q	IQR	1st Q	3rd Q	IQR	S1bm	S1am	S2bm	S2am	S1bm	S1am	S2bm	S2am
Acesulfame	-0.018	0.019	0.036	-0.001	0.020	0.022	-0.018	0.022	0.039	-0.007	0.014	0.021	725	85	253	114	0%	2%	1%	3%
1H-Benzotriazole	-0.015	0.009	0.024	-0.014	0.026	0.040	-0.013	0.013	0.027	-0.005	0.020	0.024	(-122)	117	(-221)	137	-3%	2%	-1%	3%
Bezafibrate	-0.006	0.037	0.043	0.001	0.054	0.053	-0.017	0.023	0.039	-0.017	0.031	0.048	49	28	98	153	6%	7%	3%	2%
Carbamazepine	-0.010	0.013	0.022	-0.009	0.022	0.031	-0.003	0.018	0.022	-0.007	0.012	0.020	323	94	116	200	1%	2%	3%	2%
10,11-Dihydro-10,11-dihydroxy Carbamazepine	-0.015	0.013	0.028	-0.015	0.030	0.044	-0.011	0.028	0.039	-0.011	0.018	0.029	211	108	82	527	1%	2%	4%	1%
Carbamazepine-10,11-Epoxide	-0.031	0.042	0.073	-0.044	0.089	0.133	-0.044	0.041	0.085	-0.021	0.054	0.075	61	71	(-246)	37	5%	3%	-1%	10%
Diclofenac	-0.031	0.056	0.087	0.012	0.091	0.079	-0.029	0.034	0.063	-0.009	0.043	0.052	37	16	(-222)	35	8%	12%	-1%	10%
4-Hydroxydiclofenac	-0.063	0.128	0.191	-0.023	0.281	0.304	-0.127	0.039	0.166	-0.031	0.116	0.147	52	3	(-16)	24	6%	48%	-21%	15%
Hydrochlorothiazide	-0.005	0.020	0.025	0.017	0.069	0.052	-0.005	0.032	0.037	0.003	0.037	0.034	93	18	87	32	3%	11%	4%	11%
Chlorothiazide	-0.034	0.026	0.060	-0.032	0.056	0.088	-0.013	0.041	0.053	-0.016	0.025	0.041	(-43)	(-78)	39	(-1282)	-7%	-3%	8%	0%
Irbesartan	-0.022	0.022	0.044	-0.011	0.036	0.046	-0.024	0.014	0.038	-0.004	0.019	0.023	(-111)	64	(-494)	73	-3%	3%	-1%	5%
Metformin	-0.035	0.026	0.061	-0.004	0.028	0.032	-0.017	0.021	0.038	-0.008	0.022	0.030	245	43	133	134	1%	5%	2%	3%
Guanylurea	-0.006	0.020	0.026	0.015	0.040	0.025	-0.004	0.026	0.030	-0.003	0.019	0.022	119	26	51	103	3%	8%	6%	4%
Metoprolol	0.015	0.056	0.040	0.006	0.041	0.035	-0.010	0.022	0.031	0.001	0.024	0.024	18	27	112	66	16%	8%	3%	6%
α-Hydroxymetoprolol	0.014	0.058	0.043	0.003	0.091	0.087	-0.018	0.048	0.065	-0.003	0.038	0.041	22	15	26	33	14%	13%	12%	12%
Metoprolol Acid	-0.068	-0.019	0.049	-0.087	0.007	0.094	-0.036	0.035	0.071	-0.033	0.000	0.032	(-15)	(-27)	(-96)	(-41)	-23%	-8%	-3%	-10%
Sitagliptin	-0.020	0.029	0.050	0.005	0.028	0.022	-0.024	0.033	0.056	-0.003	0.014	0.017	118	46	44	189	3%	5%	7%	2%
Sotalol	-0.018	0.018	0.036	-0.022	0.038	0.060	-0.011	0.017	0.029	-0.007	0.022	0.029	(-118)	38	138	103	-3%	5%	2%	4%
Sulfamethoxazole	-0.044	0.138	0.182	-0.041	0.088	0.129	-0.145	-0.016	0.129	-0.061	0.038	0.100	38	22	(-10)	(-268)	10%	9%	-32%	-2%
Tramadol	-0.013	0.014	0.027	-0.013	0.029	0.042	-0.007	0.017	0.024	-0.008	0.016	0.024	(-1129)	54	237	154	0%	4%	1%	2%
Valsartan	0.008	0.045	0.037	0.007	0.042	0.035	-0.004	0.028	0.032	0.005	0.031	0.026	24	34	53	43	12%	6%	6%	8%
Valsartan Acid	-0.052	-0.007	0.045	-0.050	-0.009	0.041	-0.036	-0.001	0.035	-0.021	0.010	0.031	(-22)	(-23)	(-33)	(-76)	-15%	-10%	-9%	-5%
Venlafaxine	-0.013	0.046	0.059	-0.017	0.027	0.044	-0.030	0.056	0.085	-0.002	0.018	0.020	68	149	(-2401)	122	4%	1%	0%	3%
O-Desmethylvenlafaxine	-0.016	0.022	0.037	-0.006	0.026	0.032	-0.016	0.012	0.028	-0.008	0.014	0.022	138	90	(-1578)	360	2%	2%	0%	1%

Relation of attenuation processes to most relevant environmental conditions in River Erpe

Photolysis

Photolysis of TrOCs (both direct and indirect) is expected to be driven by diurnal fluctuations[8] of solar radiation within sampling-periods and changes in intensity of solar radiation between sampling periods. According to Schwarzenbach et al.[9] the first order rate constant of direct photolysis (k_p) for a specific compound is described by the product of the reaction quantum yield $\Phi_{ir}(\lambda)$, a measure for the number of molecules transformed per photons absorbed, and the rate of light absorption $k_a(\lambda)$. The latter is linearly related to the light intensity W(λ). However, all those measures are wavelength (λ) dependent. Hence, assuming a perfectly mixed water body and a homogenous light attenuation as well as disregarding indirect photolysis, the degradation rate of a compound that is only affected by photolysis would be linearly related to solar radiation intensity at a specific wavelength. As the solar radiation is a lumped value for the sum of intensities though and the ratio of wavelengths (e.g. UVA and UVB) in the total intensity changes within the course of a day, the solar radiation measured in the present study cannot be linearly related to the degradation rates and Spearman correlation coefficients are appropriate.[8] In addition extend of shading by tree canopy or macrophytes will likely affect the influence of solar radiation. The latter two factors vary spatially (higher abundance of macrophytes in less shaded areas) and temporally (seasonal changes in canopy and macrophyte growth, as well as macrophyte mowing). As indirect photolysis can-not be disregarded, DOC and nitrate concentration as potential photosensitiser have to be considered.[10,11] Although DOC concentration (11.6 ± 1.4 mg L^{-1}) and nitrate concentrations (7.1 ± 0.8 mg L^{-1}) in river Erpe are relatively high, differences between sampling situations and diurnal fluctuations are assumed to be of minor importance compared to fluctuation in solar radiation for net-photolysis of photosensitive compounds (

Table S1).

$$-\left(\frac{dC_i}{dt}\right)_{p,\lambda} = \Phi_{ir}(\lambda)\mathrm{k}_a(\lambda)\mathrm{C}_i = \mathrm{k}_p(\lambda)\mathrm{C}_i$$

Biodegradation

Biodegradation is more complex due to the variable nature of microbial communities and (co-) metabolic degradation processes.[12] However, the composition of communities are assumed to be rather constant in diversity and processes due to the constantly high proportion of treated wastewater in River Erpe. Hotspots of biodegradation occur mainly at ecohydrological interfaces, i.e. in biofilms at the surface of submerged macrophytes or in the hyporheic zone.[13] Hence, biodegradation is spatially variable, due to heterogeneous flow regimes and sediment properties and also temporally due to changing presence of macrophytes. In addition, microbial activity is sensitive to temperature as respiration and carbon consumption of microbial communities is closely positive related to temperature.[14] Temperature is seen as one of the major control of biogeochemical processing. It influences microbial activity in different ways. Higher temperatures promote e.g. reaction rates, viscosity, bioavailability, nutrient uptake and can even alter the composition of a microbial community. [15] Water temperature was shown to be particularly related to respiration and carbon consumption.[14] Variation in biodegradation rates of organic contaminants with diurnal changes in temperature in soil were reported previously.[15] Comer-Warner et al.[16] showed an increase in sediment respiration with increasing temperature depending on the sediment type. Hence, we can

expect that the diurnal fluctuations in water temperature will influence biodegradation rates in the stream. Availability of nutrients and redox-conditions are additional factors that influence microbial activity.[17,18] However, due to high concentrations of nutrients, microbial activity is expected to not be nutrient-limited. The turbulences caused by the fish-ladders are expected to cause relatively high saturation of the water column with oxygen and only shallow hyporheic exchange in the oxygenated zone of the streambed is expected to contribute to in-stream attenuation.[19] So aerobic respiration is expected to be the prevailing biodegradation process contributing to in-stream attenuation.

Sorption

Removal rates of neutral and negatively charged TrOCs (at ambient pH) in the sediment of River Erpe were discussed to be not considerably affected by sorption due to their low log D_{OW}.[19,20] The compound of highest log D_{OW} in the study of Schaper et al.[19] was carbamazepine (2.77), which showed now significant removal in the sediment profile. The only compound exhibiting a higher log D_{OW} in the present study is irbesartan (5.98) (Table S8). Hence, for irbesartan a contribution of sorption onto organic matter to attenuation must be considered. However, median k_{att} of irbesartan were comparably low (close to 0.01 h^{-1}). Writer et al.[21] found a relation of pKa of compounds to their attenuation rate in column studies. No such relation was seen in the present study (Table S7). In addition, Acuña et al.[22] found no relation between log K_{OW} and the mass transfer coefficients, but a significant relation between the log K_{OW} and the coefficients of variation of the mass transfer coefficients in the four rivers of the study (pearson r=-0.63, P<0.05). In the present study, neither median k_{att} nor the interquartile range of the k_{att} distributions (Table S8) showed significant Pearson-correlation (P>0.05) to log K_{OW} or log D_{OW} (Table S7).

Table S7 Pearson's correlation coefficient r and 2-tailed p-value of median k_{att} and interquartile range (IQR) vs. K_{OW}, D_{OW} and pKa

	S1bm		S1am		S2bm		S2am	
	r	**P-value**	**r**	**P-value**	**r**	**P-value**	**r**	**P-value**
Median k_{att} vs. K_{OW}	0.28	0.18	0.24	0.25	-0.19	0.38	0.31	0.14
IQR k_{att} vs. K_{OW}	0.18	0.40	0.18	0.41	0.13	0.55	0.20	0.35
Median k_{att} vs. D_{OW}	0.29	0.18	0.12	0.58	-0.05	0.80	0.20	0.35
IQR k_{att} vs. D_{OW}	0.05	0.81	0.16	0.46	0.15	0.48	0.13	0.54
Median k_{att} vs. pKa	0.02	0.93	-0.17	0.43	0.16	0.45	-0.20	0.36
IQR k_{att} vs. pKa	-0.14	0.50	-0.28	0.18	-0.17	0.43	-0.31	0.14

Kunkel and Radke[23] assumed, that sorption generally does not affect TrOC in WWTP-effluent dominated rivers due to the continuous exposure of potential binding sites to high concentrations in sorptives. However, in other studies, sorption has been suggested to be the main in-stream removal process for certain positively charged compounds.[21,24] Sediment organic matter, clay particles and biofilm provide predominantly negatively charged binding sites.[20,21,25] Hence, in the present study sorption of compounds that are positively charged under the prevailing pH 7.8 needs to be considered as an attenuation process. Similar to biodegradation, sorption is influenced by the availability of ecohydrological interfaces. Therefore, changes in macrophyte abundance and differences in hyporheic exchange might lead to differences in attenuation of TrOC sensitive to sorption processes.

Table S8 Therapeutic class and Log K_{OW} of analysed compounds as reported in Posselt et al.[3] pKa, log D_{OW} and charge values were obtained from the online platform Chemicalize (https://chemicalize.com/)

Compound (parent compounds are highlighted in bold, related TPs are listed below)	Therapeutic class	Strongest basic pKa	Log K_{OW}	Log D_{OW} (pH 7.8)	Charge of most abundant species (pH 7.8)
Acesulfame	artificial sweetener	3.02	-0.55	-1.49	anionic
1H-Benzotriazole	corrosion inhibitor	0.6	1.25	1.24	neutral
Bezafibrate	lipid regulator	-0.84	3.99	0.59	anionic
Carbamazepine	anticonvulsant	-3.8	2.77	2.77	neutral
10,11-Dihydro-10,11-dihydroxy Carbamazepine	TP of carbamazepine	-	1.26	0.65	anionic
Carbamazepine-10,11-Epoxide	TP of carbamazepine	3.65	2.58	0.52	anionic
Diclofenac	NSAID analgesic	-2.1	4.26	0.91	anionic
4-Hydroxydiclofenac	TP of diclofenac	-0.59	3.96	0.48	anionic
Hydrochlorothiazide	diuretic	-2.7	-0.58	-0.58	neutral
Chlorothiazide	(diuretic), TP of hydrochlorothiazide	1.15	-0.44	-0.46	neutral
Irbesartan	angiotensin II receptor antagonist	4.12	5.98	4.09	anionic
Metformin	antihyperglycemic agent	12.33	-0.92	-5.47	cationic
Guanylurea	TP of metformin	9.79	-2.03	-3.69	cationic
Metoprolol	β-blocker	9.67	1.8	-0.10	cationic
α-Hydroxymetoprolol	TP of metoprolol	9.67	0.84	-0.726	cationic
Metoprolol Acid	TP of metoprolol	3.54	-1.24	-1.24	zwitter
Sitagliptin	antihyperglycemic agent	8.78	1.26	0.23	cationic
Sotalol	β-blocker	9.43	-0.4	-1.75	cationic
Sulfamethoxazole	antibiotic	1.97	0.79	-0.08	anionic
Tramadol	opioid analgesic	9.23	2.45	1.01	cationic
Valsartan	angiotensin II receptor antagonists	-0.64	5.27	0.66	anionic
Valsartan Acid	TP of valsartan	-1.45	3.18	-1.60	anionic
Venlafaxine	antidepressant	8.91	2.74	1.6	cationic
O-Desmethylvenlafaxine	TP of venlafaxine	8.87	2.29	1.45	cationic

Limitations of the study

The measurements and calculations applied in the present study are associated with different uncertainties and simplifications. Using first order kinetics to calculate attenuation is a great simplification, as the reality for many compounds is likely a combination of formation and degradation through different pathways and processes. Distinguishing these pathways for each individual compound is out of the scope of this study. Hence, the rate constants are a proxy to estimate a net-removal combining all processes. Especially in cases where negative net-removal, and thus formation was found (e.g. valsartan acid and metoprolol acid) the negative constants are not indicators of an actual process but rather a means to obtain comparable values. In addition, using merely two concentrations to obtain a rate constant introduces certain errors due to measurement uncertainties. Uncertainties in k_{att} caused by measurement uncertainties in the concentration of each compound combined with the uncertainty of boron concentrations are shown in Table S8. Compounds that depict more than 50% of parcels with k_{att} above the uncertainty (4-hyroxydiclofenac, hydrochlorothiazide, guanylurea, metoprolol, metoprolol acid, valsartan, valsartan acid) and related compounds (TPs and parent compounds) are presumed most relevant and

thus discussed in this study. In addition, the travel times estimation contains uncertainties that affect the k_{att} calculation. Also the travel times likely changed during the study periods which was not accounted for. Furthermore, only a selection of environmental parameters that potentially influence the fate of TrOCs was measured or estimated.

Table S9 Uncertainties of k_{att} calculated by uncertainty propagation of measurement precisions (% relative standard deviation RSD) of $C_{x,i,in}$, $C_{x,i,out}$, $C_{ref,i,in}$ and $C_{ref,i,out}$ in Equ. 1. Bold values indicate where more than 50% of parcels show k_{att} exceed the uncertainty. Inter-day instrumental precision was calculated from quality controls (n= 4). Limits of detection (LOD) and limits of quantification (LOQ) in Erpe-water matrix as reported in Posselt et al.[3]

Compound (parent compounds are highlighted in bold, related TPs are listed below)	**Inter-day instrumental Precision (%RSD)**	**Uncertainties k_{att} [h^{-1}]**				**LOD [µg L^{-1}]**	**LOQ [µg L^{-1}]**
		S1bm	**S1am**	**S2bm**	**S2am**		
Acesulfame	2.0	±0.012	±0.017	±0.012	±0.010	0.018	0.088
1H-Benzotriazole	2.7	±0.011	±0.015	±0.011	±0.009	0.005	0.114
Bezafibrate	2.9	±0.035	±0.050	±0.035	±0.029	0.024	0.094
Carbamazepine	6.6	±0.030	±0.043	±0.029	±0.024	0.025	0.025
10,11-Dihydro-10,11-dihydroxy Carbamazepine	9.0	±0.030	±0.042	±0.029	±0.024	0.02	0.088
Carbamazepine-10,11-Epoxide	7.1	±0.119	±0.169	±0.116	±0.097	0.006	0.03
Diclofenac	6.0	±0.031	±0.043	±0.030	±0.025	0.107	0.383
4-Hydroxydiclofenac	16.5	±0.080	**±0.113**	±0.078	±0.065	0.015	0.05
Hydrochlorothiazide	5.7	±0.018	**±0.026**	±0.018	**±0.015**	0.044	0.151
Chlorothiazide	17.9	±0.023	±0.033	±0.023	±0.019	0.019	0.082
Irbesartan	2.7	±0.023	±0.033	±0.023	±0.019	0.008	0.029
Metformin	3.7	±0.014	±0.020	±0.014	±0.012	0.119	0.394
Guanylurea	1.5	±0.008	**±0.011**	**±0.008**	**±0.006**	0.329	1.298
Metoprolol	4.2	**±0.012**	**±0.017**	±0.012	**±0.010**	0.006	0.085
α-Hydroxymetoprolol	18.3	±0.092	±0.131	±0.090	±0.075	0.067	0.365
Metoprolol Acid	5.3	**±0.018**	**±0.025**	±0.017	**±0.014**	0.014	0.06
Sitagliptin	9.9	±0.068	±0.097	±0.067	±0.056	0.01	0.03
Sotalol	7.4	±0.020	±0.029	±0.020	±0.016	0.017	0.092
Sulfamethoxazole	2.7	±0.076	±0.108	±0.075	±0.062	0.01	0.047
Tramadol	2.3	±0.012	±0.017	±0.012	±0.010	0.003	0.098
Valsartan	11.4	**±0.010**	**±0.015**	**±0.010**	**±0.008**	0.049	0.049
Valsartan Acid	7.9	**±0.021**	**±0.029**	**±0.020**	±0.017	0.114	0.372
Venlafaxine	3.3	±0.018	±0.026	±0.018	±0.015	0.01	0.01
O-Desmethylvenlafaxine	4.8	±0.055	±0.078	±0.054	±0.045	0.017	0.063

References

(1) Lewandowski, J.; Putschew, A.; Schwesig, D.; Neumann, C.; Radke, M., Fate of organic micropollutants in the hyporheic zone of a eutrophic lowland stream: results of a preliminary field study. *Sci Total Environ* **2011,** *409*, (10), 1824-35.
(2) Kilpatrick, F. A.; Wilson, J. F., *Measurement of time of travel in streams by dye tracing*. US Government Printing Office: 1989.
(3) Posselt, M.; Jaeger, A.; Schaper, J.; Radke, M.; Benskin, P., Determination of polar organic micropollutants in surface and pore water by high-resolution sampling-direct injection-ultra high performance liquid chromatography-tandem mass spectrometry. *(submitted)* **2018**.
(4) Woerman, A., Comparison of models for transient storage of solutes in small streams. *Water Resources Research* **2000,** *36*, (2), 455-468.
(5) Cirpka, O. A.; Fienen, M. N.; Hofer, M.; Hoehn, E.; Tessarini, A.; Kipfer, R.; Kitanidis, P. K., Analyzing Bank Filtration by Deconvoluting Time Series of Electric Conductivity. *Groundwater* **2007,** *45*, (3), 318-328.
(6) Charriau, A.; Lissalde, S.; Poulier, G.; Mazzella, N.; Buzier, R.; Guibaud, G., Overview of the Chemcatcher® for the passive sampling of various pollutants in aquatic environments Part A: Principles, calibration, preparation and analysis of the sampler. *Talanta* **2016,** *148*, 556-571.
(7) Moschet, C.; Vermeirssen, E. L. M.; Singer, H.; Stamm, C.; Hollender, J., Evaluation of in-situ calibration of Chemcatcher passive samplers for 322 micropollutants in agricultural and urban affected rivers. *Water Research* **2015,** *71*, 306-317.
(8) Hanamoto, S.; Nakada, N.; Yamashita, N.; Tanaka, H., Modeling the photochemical attenuation of down-the-drain chemicals during river transport by stochastic methods and field measurements of pharmaceuticals and personal care products. *Environ Sci Technol* **2013,** *47*, (23), 13571-7.
(9) Schwarzenbach, R. P.; Gschwend, P. M.; Imboden, D. M., Direct Photolysis. In *Environmental Organic Chemistry*, John Wiley & Sons, Inc.: 2005; pp 611-654.
(10) Schwarzenbach, R. P.; Gschwend, P. M.; Imboden, D. M., Indirect Photolysis: Reactions with Photooxidants in Natural Waters and in the Atmosphere. In *Environmental Organic Chemistry*, John Wiley & Sons, Inc.: 2005; pp 655-686.
(11) Wang, Y.; Roddick, F. A.; Fan, L., Direct and indirect photolysis of seven micropollutants in secondary effluent from a wastewater lagoon. *Chemosphere* **2017,** *185*, 297-308.
(12) Schwarzenbach, R. P.; Gschwend, P. M.; Imboden, D. M., Biological Transformations. In *Environmental Organic Chemistry*, John Wiley & Sons, Inc.: 2005; pp 687-773.
(13) Krause, S.; Lewandowski, J.; Grimm, N. B.; Hannah, D. M.; Pinay, G.; McDonald, K.; Martí, E.; Argerich, A.; Pfister, L.; Klaus, J.; Battin, T.; Larned, S. T.; Schelker, J.; Fleckenstein, J.; Schmidt, C.; Rivett, M. O.; Watts, G.; Sabater, F.; Sorolla, A.; Turk, V., Ecohydrological interfaces as hot spots of ecosystem processes. *Water Resources Research* **2017,** *53*, (8), 6359-6376.
(14) Jude, K. A.; Giorgio, P. A. d.; Kemp, W. M., Temperature regulation of bacterial production, respiration, and growth efficiency in a temperate salt-marsh estuary. *Aquatic Microbial Ecology* **2006,** *43*, (3), 243-254.
(15) Ali, A.; Subhasis, G., Effects of diurnal temperature variation on microbial community and petroleum hydrocarbon biodegradation in contaminated soils from a sub-Arctic site. *Environmental Microbiology* **2015,** *17*, (12), 4916-4928.
(16) Comer-Warner, S. A.; Romeijn, P.; Gooddy, D. C.; Ullah, S.; Kettridge, N.; Marchant, B.; Hannah, D. M.; Krause, S., Thermal sensitivity of CO2 and CH4 emissions varies with streambed sediment properties. *Nature Communications* **2018,** *9*, (1), 2803.
(17) Velázquez, Y. F.; Nacheva, P. M., Biodegradability of fluoxetine, mefenamic acid, and metoprolol using different microbial consortiums. *Environmental Science and Pollution Research* **2017,** *24*, (7), 6779-6793.
(18) Schmidt, N.; Page, D.; Tiehm, A., Biodegradation of pharmaceuticals and endocrine disruptors with oxygen, nitrate, manganese (IV), iron (III) and sulfate as electron acceptors. *J. Contam. Hydrol.* **2017,** *203*, 62-69.

(19) Schaper, J. L.; Seher, W.; Nutzmann, G.; Putschew, A.; Jekel, M.; Lewandowski, J., The fate of polar trace organic compounds in the hyporheic zone. *Water Res* **2018,** *140*, 158-166.
(20) Tülp, H. C.; Fenner, K.; Schwarzenbach, R. P.; Goss, K.-U., pH-Dependent Sorption of Acidic Organic Chemicals to Soil Organic Matter. *Environ. Sci. Technol.* **2009,** *43*, (24), 9189-9195.
(21) Writer, J. H.; Antweiler, R. C.; Ferrer, I.; Ryan, J. N.; Thurman, E. M., In-Stream Attenuation of Neuro-Active Pharmaceuticals and Their Metabolites. *Environ. Sci. Technol.* **2013,** *47*, (17), 9781-9790.
(22) Acuña, V.; von Schiller, D.; García-Galán, M. J.; Rodríguez-Mozaz, S.; Corominas, L.; Petrovic, M.; Poch, M.; Barceló, D.; Sabater, S., Occurrence and in-stream attenuation of wastewater-derived pharmaceuticals in Iberian rivers. *Sci. Total Environ.* **2015,** *503–504*, 133-141.
(23) Kunkel, U.; Radke, M., Fate of pharmaceuticals in rivers: Deriving a benchmark dataset at favorable attenuation conditions. *Water Research* **2012,** *46*, (17), 5551-5565.
(24) Riml, J.; Wörman, A.; Kunkel, U.; Radke, M., Evaluating the fate of six common pharmaceuticals using a reactive transport model: Insights from a stream tracer test. *Sci. Total Environ.* **2013,** *458–460*, 344-354.
(25) Torresi, E.; Polesel, F.; Bester, K.; Christensson, M.; Smets, B. F.; Trapp, S.; Andersen, H. R.; Plósz, B. G., Diffusion and sorption of organic micropollutants in biofilms with varying thicknesses. *Water Research* **2017,** *123*, 388-400.